

PAPER • OPEN ACCESS

Universality of delay-time averages for financial time series: analytical results, computer simulations, and analysis of historical stock-market prices

To cite this article: Stefan Ritschel *et al* 2021 *J. Phys. Complex.* **2** 045003

View the [article online](#) for updates and enhancements.

You may also like

- [Economic Impact Assessment of the Dual-track Electricity Price System in China](#)
Weibin Ding, Feng Gao, Yang Xu et al.
- [Asymmetric Price Transmission in the Indonesian Food Market](#)
Fitrotul Laili, Wiwit Widyawati and Putri Budi Setyowati
- [Sending out an SOS: using start of rainy season indicators for market price forecasting to support famine early warning](#)
Frank M Davenport, Shraddhanand Shukla, William Turner et al.

OPEN ACCESS

PAPER

RECEIVED
26 June 2021REVISED
16 August 2021ACCEPTED FOR PUBLICATION
27 August 2021PUBLISHED
13 October 2021

Original content from this work may be used under the terms of the [Creative Commons Attribution 4.0 licence](#).

Any further distribution of this work must maintain attribution to the author(s) and the title of the work, journal citation and DOI.



Universality of delay-time averages for financial time series: analytical results, computer simulations, and analysis of historical stock-market prices

Stefan Ritschel^{1,*}, Andrey G Cherstvy^{1,2,*} and Ralf Metzler^{1,*} ¹ Institute for Physics and Astronomy, University of Potsdam, 14476 Potsdam-Golm, Germany² Institut für Physik, Humboldt-Universität zu Berlin, 12489 Berlin, Germany

* Authors to whom any correspondence should be addressed.

E-mail: ritschel_stefan@yahoo.de, a.cherstvy@gmail.com and rmetzler@uni-potsdam.de**Keywords:** econophysics, geometric Brownian motion, time-series analysis

Abstract

We analyze historical data of stock-market prices for multiple financial indices using the concept of delay-time averaging for the financial time series (FTS). The region of validity of our recent theoretical predictions [Cherstvy A G *et al* 2017 *New J. Phys.* **19** 063045] for the standard and delayed time-averaged mean-squared ‘displacements’ (TAMSDs) of the historical FTS is extended to all lag times. As the first novel element, we perform extensive computer simulations of the stochastic differential equation describing geometric Brownian motion (GBM) which demonstrate a quantitative agreement with the analytical long-term price-evolution predictions in terms of the delayed TAMSD (for all stock-market indices in crisis-free times). Secondly, we present a robust procedure of determination of the model parameters of GBM via fitting the features of the price-evolution dynamics in the FTS for stocks and cryptocurrencies. The employed concept of single-trajectory-based time averaging can serve as a predictive tool (proxy) for a mathematically based assessment and rationalization of probabilistic trends in the evolution of stock-market prices.

1. Introduction

1.1. Evolution of stock-market prices and stochastic processes with multiplicative dynamics

Variations of stock-market prices are generally believed to be unpredictable, with *completely random* price fluctuations obeying memory-less random walks [1–4]. This was first argued in 1900 by Bachelier [1], who introduced (before Einstein and Langevin) the concept of arithmetic Brownian motion (BM), developed further in 1908 by Bronzin [2]. Bachelier and Bronzin laid the foundation of modern financial mathematics, the starting point for applying stochastic processes and statistical analysis to time-evolution of stock prices, $S(t)$. Generations of brilliant scientists—economists, econometricians, econophysicists, specialists of financial-time-series (FTS) analysis, etc (including many Nobel-prize winners)—have been focusing their long-term efforts on unraveling the general underlying functioning principles of financial markets and predicting the governing laws of formation and evolution of asset prices [1–45] (see also the key books [46–63]). One of the main conjectures for financial-market models is that consecutive price changes and respective returns, $r_n = [S(t_n) - S(t_{n-1})]/S(t_{n-1})$, are uncorrelated in time (Bachelier’s first law [1]) and can be represented by independent identically distributed Gaussian random variables.

The ground-breaking discovery in financial mathematics was the development of the paradigmatic geometric BM (GBM) process (also called ‘exponential’ or ‘economic’ BM). It was ‘revived’ in 1965 by Samuelson [12] from Bachelier’s works and the respective closed-form option-pricing formula utilizing the GBM process was invented by Black, Scholes, and Merton (BSM) in 1973 [21–26]. This famous BSM model was generalized i.a., by Cox, Ingersoll, and Ross [32], Hull and White [33], Wiggins [J B Wiggins, Option values under stochastic volatility: theory and empirical estimates, *J. Financial Econ.*, **19**, 351 (1987)], Stein and Stein

[E M Stein and J C Stein, Stock price distributions with stochastic volatility: an analytic approach, *Rev. Financial Studies*, 4, 727 (1991)], and later by Heston [36] who presented the asset-price-evolution formula in the presence of stochastic volatility or ‘riskiness’ (see also references [23, 28, 31, 32, 64] for models of time-varying and price-dependent volatility^{3,4}). In the BSM model, the evolution of asset prices obeys GBM with a log-normal distribution of prices and $\log[\text{price}(\text{time})]$ increasing roughly linearly with time (see also section 3.1). The models of jump-diffusion [25, 28, 41, 66–71], square-root [32] diffusion, time-changed, and alternative [28, 72–75] stochastic processes for option pricing were proposed as well.

The exponential growth of stock-market prices—that appears to be consistent with many GBM-based models—is at the core of a highly speculative [76] (as mentioned already by Bachelier [1]) stock-price-formation process. The quickest price and profit growth [77–79] is also attributable to commodity-oriented (oil, gold, etc) [80], housing and real-estate [81] markets, and, in particular, cryptocurrencies [82–84] as well as other financial pyramids⁵. We refer the reader to the reviews [78, 86] for the basic concepts of economics (including volatility, economic crashes, and human behavior) as well as mathematical models/approaches in modern finance.

Despite a number of inherent limitations and idealizations of the BSM-based model [87, 88] and certain claims that option-traders rarely [65, 85] use it as their main decision-making strategy (employing complicated heuristic/empirical models instead), the interest to GBM-type models from the community of stochastic processes stays persistent [89–91]. Mathematically, numerous extensions of GBM and BSM model were developed (the list of studies is too long to adequately overview it here), including, i.a., pricing of lookback and barrier options, options with constant elasticity of variance, GBM modifications based on fractional equations, stochastic volatility, with anomalous-diffusion processes [92–101], and subordination [102, 103]. The concept of (subdiffusive) continuous-time random walks was also employed [104, 105] to describe periods of price stagnation in FTS (as ‘trapping events’ with distributed waiting times) [106–108]. Some aspects of (non)-ergodicity [109–111] were also studied for GBM [112, 113] and discussed for economics in general [114–117].

As no statistical ensemble of ‘independent’ FTS can be obtained at identical and controlled conditions, no reproducible ‘economic experiments’ can in principle be conducted to probe other possible price-evolution scenarios. The absence of ensemble averaging as such—the nonexistence of the ensemble-averaged mean-squared ‘displacement’ (MSD)—undoubtedly favors the single-trajectory-based approaches for the FTS-analysis. Here, the ‘moving average’ and exponentially-weighted moving average are often used to smoothen the price trends and optimize profits for certain trading strategies employing price fluctuations around those averages.

1.2. Market efficiency, cost of information, and behavioral finance

The mathematical models of GBM-type—the main focus of our analytical analysis—clearly oversimplify the behavior of real financial markets. The space of factors and parameters affecting actual price variations of a stock/asset is huge and below we shortly overview some mechanisms of price-formation processes.

The response of markets to financial news, relevant judicial decisions, and macroeconomic announcements [3, 5, 86, 118, 119] in terms of reaching an ‘equilibrium’ via fluctuations and price-formation processes is neither exactly defined nor reproducible [120]. This process involves aspects of information spreading, numerous feedback mechanisms, principles of *behavioral finance* [121–125] (including beliefs [115], expectations, overconfidence, heterogeneity of traders [115, 126], gambling behavior, speculation, reaction to trends and rumors, ‘magical thinking’ [122], etc). In a hypothetical scenario of perfectly efficient, infinitely ‘liquid’ and memory-less markets—with all relevant information being publicly available and instantly reflected in the current price

³ A contract entitling its holder (with no obligation) to buy an underlying asset at a preset price on a given date in the future is a ‘call’ option (American-type). This is ‘striking’ or ‘exercise’ price, while the expiration date is the maturity time of the option [18, 22, 23]. The goal is to price an asset/derivative provided the strike price and expiration date are known (to sell it with profit upon expiration). The BSM model is the general framework to attack this goal, working backward in time to assess option prices. In contrast, a contract that entitles its holder to sell a given asset or share at any time on or before expiration is called a ‘put’ option (American-type) [22, 23]. European-type options differ by the fact that they cannot be exercised before the last day of the contract.

⁴ From a historical perspective, similar option-price-valuation formulas were discussed by Bronzin in 1908 [2], Sprengle in 1961 [8], Boness in 1964 [11], Samuelson in 1965 [12, 18], and Thorp in 1969 [17] (see the discussion by Haug and Taleb [65] and the BSM story by Black [26]). We also refer to the bond-pricing model by Cox et al [32], considered also in the presence of inflation.

⁵ The Dutch tulip mania of 1636–1637 is the first known speculative bubble. The rational market principles fail at the times of financial crises (either of 1873 and 1893 panics, the ‘great crash’ of 1929 (‘Black Friday’), the ‘Black-Monday’ of 1987, the 1998–1999 Russian financial crisis, the 2000 Dot-Com bubble, the 2008–2009 financial crisis, the BitCoin crash late December 2017, and the economic decline/crash caused by rapidly growing Covid-19 pandemic uncertainties in March–April 2020, etc). These crises—often inevitable, expected but almost unpredictable ‘Black-Swan’-like [85] events—are needed i.a. to reload the ‘price-growth spring’ via regaining the confidence of investors in a given stock (e.g., after its ‘rebranding’, splitting, merging, etc).

[3]—even a tax-free trading would be hardly profitable. Real financial markets are extremely complex and out-of-equilibrium systems [86], often operating at a limited ‘liquidity’. Thus, some short-horizon trends of price evolution may potentially be predictable from the incoming information and based on statistical analyses of price-fluctuation patterns of market response to similar information in the past.

The traders’ anticipation, numerous sources and types of noise [120], delays and memories are existential for trading and ‘functioning’ of the market. In traditional economic theories, the trading events act as an instrument to dynamically probe and approach the market equilibrium (Walras’ *tâtonnement* process, see reference [86]), via regulating supply and demand [86]. This equilibrium can, however, be illusive or even artificially created, e.g., by ‘big players’ controlling the market [115]. These (usually much more informed investors) trade profitably knowing the ‘true price’ [35, 115, 118, 120, 127], often at the expense of less informed traders [128].⁶ The cost of information acquisition prevents the market from being ‘informationally efficient’ [118, 129, 130] impeding (or even destroying) the ‘fair play’ among the participants and often violating the market-efficiency hypothesis.

As an indication of private-information-driven changes of volatility, the fluctuations of FTS were demonstrated (over multiple time domains) to be far too large [131], and with price changes being only partially attributable to important financial news [127, 132]. The variations of stock-market prices were also shown to fail in reflecting rationally changes in fundamental values [133]. This questions the relative role of exogenous (external) versus endogenous fluctuations (or ‘self-generated’ price changes) in such price-formation processes. The latter are often irrational and affected possibly more by behavioral-finance principles and human decision-making principles, rather than by real values.

Long-term speculative exponential GBM-like growth of stock-market prices is, thus, supplemented by disproportionately volatile and often irrational short-term price variations (with noise- versus information-based trends [86, 120, 134] being impossible to separate rationally). Moreover, market ‘overreaction’ to new financial information is well known [121, 135]. This can be a useful instrument for the traders to artificially create bigger winning margins first in order later to ‘capitalize’ larger profits on a price ‘bounce-back’⁷.

The exponential GBM-like price growth can, in addition, be interrupted by hardly predictable [85]—but possibly inevitable or even pre-programmed—price drops at times of market crashes and financial bubbles [80, 81, 85, 139–142]. The ‘efficient market hypothesis’ [12, 19] implies that the variation of the unanticipated part of stock prices should be a martingale [25], with no correlations in price differences [4, 12] (see also reference [136]). The speculative bubbles are based on overoptimistic expectations, the herding behavior of market participants [143–146]—particularly in periods of extreme volatilities (in high-risk–high-reward times), and pure greed—all accelerating the price dynamics and growth, with a possibly superexponential [147, 148] price ‘explosion’ near the bubble. The burst of speculative bubbles and subsequent market crashes are inconsistent with the hypothesis of efficient markets [5, 19, 27] (the empirical evidence of the latter are, in fact, insufficient [133, 136, 138, 149]).

1.3. Outline of the paper

The paper is organized as follows. In section 2 we recapitulate on the recent results of the time-averaged MSD (TAMSD) $\overline{\delta_i^2(\Delta)}$ analysis for GBM and historical stock-market prices [150]. In section 3 we present the essential details of the analytical model of GBM. In section 3.1 we introduce the formalism for GBM, in section 3.2 the key expressions for its delayed TAMSD $\overline{\delta_{d,i}^2(\Delta)}$ are derived. In section 4 we discuss the numerical solution of the stock-market price-evolution equation and present the details of computer simulations for GBM. The findings for $\overline{\delta_i^2(\Delta)}$ and $\overline{\delta_{d,i}^2(\Delta)}$ are described and compared to analytical results for GBM. In section 5 we present the main results of the FTS-analysis in terms of the delayed TAMSDs for a number of indices. In section 6 we summarize the results, list general conclusions, and discuss possible further developments.

Our main target here is to present the full analytical results for $\overline{\delta_{d,i}^2(\Delta)}$ (generalizing and extending those of reference [150]), to confirm the agreement of its behavior with the results of computer simulations and the analysis of evolution of stock-price data (at all lag times). We present some auxiliary figures in appendix A, some derivations in appendix B, and the data-driven procedure of parameters estimation in appendix C.

⁶ The latter can only react to particular news/trends, conveyed in the already-adjusted stock prices (with an unknown information context [86]), and thus predestined in a long run to make less money than the better-informed ones. No trading would likely be profitable for informed traders if all information they possess (including those on future orders or deals) were instantly publicly available.

⁷ Some correlations of price changes and certain predictability of returns also question the paradigm of stock-market prices being describable by *unbiased/random* walks [136, 137] as well as the ‘efficient market hypothesis’ itself [138]. This, in turn, indicates inefficiency of the underlying mechanisms of price formation, limiting a set of mathematical models and stochastic processes implementable to *quantitatively* describe such stock-price variations.

2. Previous results for the TAMSD of GBM: aged and delayed properties

In contrast to standard moving/‘rolling’ average—averaging prices over n preceding points along an FTS—the TAMSD operates with all points of an FTS $S_i(t)$ of length T yielding the trajectory-averaged displacements at varying values of the lag time, $0 < \Delta < T$, via integrating the squared stock-price increments as [150]

$$\overline{\delta_i^2(\Delta)} = \frac{1}{T - \Delta} \int_0^{T-\Delta} [S_i(t + \Delta) - S_i(t)]^2 dt. \quad (1)$$

Here, $S_i(t)$ is the price of the i th stock. In equation (1) the price increments shifted in time by Δ are squared and averaged over the FTS. The discrete interpretation of (1) for equidistantly sampled input data—such as in historical FTS—is straightforward. The TAMSD concept—ubiquitously used for the analysis of single-particle-tracking data [154–156]—was employed to the FTS-analysis in reference [150], a foundation for the current study. The mean TAMSD for N independent trajectories constructing a ‘satisfactory’ statistical ensemble is

$$\langle \overline{\delta^2(\Delta)} \rangle = \frac{1}{N} \sum_{i=1}^N \overline{\delta_i^2(\Delta)}. \quad (2)$$

We summarize below the basic concepts and main results of reference [150], focusing in particular on the concepts of the aged and delayed TAMSDs. First, we confirmed that the TAMSD behaved strictly linear with the lag time Δ for a large number of companies of various classes, with

$$\langle \overline{\delta^2(\Delta)} \rangle \sim \langle S^2(T) \rangle \times \Delta/T. \quad (3)$$

This behavior is consistent [150] with the predictions of the standard-GBM model highlighting, thus, weak ergodicity breaking [155] emerges for this process at short lag times, at $\Delta \ll T$. Specifically, the exponentially growing MSD for GBM (16) contrasts the linearly growing mean TAMSD in equation (3). We extend this analysis here for all lag times Δ and present nontrivial features of the TAMSD at later stages of the trajectories.

Second, we introduced the aged

$$\overline{\delta_{a,i}^2(\Delta)} = \frac{1}{T - \Delta} \int_{t_a}^{t_a+T-\Delta} [S_i(t + \Delta) - S_i(t)]^2 dt \quad (4)$$

and the delayed

$$\overline{\delta_{d,i}^2(\Delta)} = \frac{1}{T - t_d - \Delta} \int_{t_d}^{T-\Delta} [S_i(t + \Delta) - S_i(t)]^2 dt \quad (5)$$

TAMSDs and enumerated them as functions of the aging t_a and delay t_d time for a large number of FTS [150]. The modified TAMSDs (4) and (5) were also computed analytically for standard GBM with a constant volatility σ . The mean aged TAMSD was found (in the limit of short lag times, $\Delta \ll T$, and with no drift) to grow nearly exponentially with t_a both for real FTS and for GBM predictions, namely

$$\langle \overline{\delta_a^2(\Delta)} \rangle \sim \langle \overline{\delta^2(\Delta)} \rangle \times e^{\sigma^2 t_a}. \quad (6)$$

The stock-specific or ‘idiosyncratic’ factor σ_i^2 in equation (6) was, however, shown [150] to yield a spread of the distribution of $\log \left[\overline{\delta_{a,i}^2(\Delta)} / \overline{\delta_i^2(\Delta)} \right]$ when this ratio is examined as a function of aging time t_a for different stock-indices at a fixed lag time Δ . The most relevant difference between the aged and delayed TAMSDs is the fact that $\overline{\delta_{a,i}^2(\Delta)}$ assigns more ‘weight’ to the data points toward the end of FTS. This key difference yields (for often nearly exponentially growing FTS) some universal and parameter-free relations for the delayed TAMSD.

Third, the most interesting finding of reference [150] was the universal behavior predicted for the delayed TAMSDs versus t_d for all stock indices examined, with

$$\log \left[\overline{\delta_{d,i}^2(\Delta)} / \overline{\delta_i^2(\Delta)} \right] = \log \left[\langle \overline{\delta_d^2(\Delta)} \rangle / \langle \overline{\delta^2(\Delta)} \rangle \right] \sim t_d/T, \quad (7)$$

in the limit of short delay times and short lag times, at

$$\{t_d, \Delta\} \ll T. \quad (8)$$

The parameter-free master curve (7) obtained for many FTS is consistent [150] with the GBM-based solution in the same limit (8). The concept of the delayed TAMSD (5) introduced in reference [150] is, therefore, especially useful for the analysis of fast-growing FTSs and for assessing their universal parameter-free characteristic features, such as (7).

Our current analysis extends the consideration of $\overline{\delta_{d,i}^2(\Delta)}$ to the entire range of lag- and delay-times. We demonstrate, i.a., that the behavior of the later parts of the log $\left[\frac{\overline{\delta_{d,i}^2(\Delta)}}{\overline{\delta_i^2(\Delta)}}\right]$ versus t_d curves with a faster-than-linear growth are not inaccuracies of the basal law (7) observed at short lag times. This ‘nonlinear’ growth is rather a real feature of FTS, which agrees with both the GBM predictions and results of computer simulations, as shown below. We also clarify the implications of financial crashes on deviations from typical GBM-based evolution of FTS observed for the TAMSD in crisis-free times.

3. Model and analytical results

3.1. GBM: equation, general solution, model parameters, and moments

Since Bachelier [1], the evolution of *a priori* uncorrelated [3] stock-market prices is described using the concept of random walks. According to the BSM model, the asset price $S(t)$ obeys a stochastic differential equation driven by multiplicative [152] noise,

$$dS(t) = \mu S(t)dt + \sigma S(t) \times dW(t), \quad (9)$$

where $W(t)$ is the standard Wiener process defined via zero-mean white Gaussian noise $\xi(t)$ as

$$W(t) = \int_0^t \xi(t')dt'. \quad (10)$$

Equation (9) is considered in the Itô formalism. The constant parameters μ and σ denote the drift and volatility of this process, respectively (see the discussion in section 6.2). After applying Itô’s lemma [57, 153], one can derive from (9) the partial differential equation yielding the Black–Scholes formula (the BSM model). The solution of equation (9) in Itô representation defines GBM as a Markovian process (exponential of BM $X(t)$) of the form

$$S(t) = S_0 e^{(\mu - \sigma^2/2)t + \sigma W(t)}, \quad (11)$$

where $S_0 \equiv S(0)$ is the initial price, and

$$S(t)/S_0 \sim e^{X(t)}. \quad (12)$$

The first and second moments of GBM, defined as

$$\langle S^q(t) \rangle = \int_0^\infty S^q(t) P(S, t) dS, \quad q = \{1, 2\}, \quad (13)$$

are obtained via averaging (11) with the log-normal distribution⁸ [22, 23]

$$P(S(t), t | S_0, 0) = \frac{\exp\left(-\frac{[\log[S(t)/S_0] - (\mu - \sigma^2/2)t]^2}{2\sigma^2 t}\right)}{\sqrt{2\pi\sigma^2 S(t)^2 t}}. \quad (14)$$

The latter satisfies the Fokker–Planck-like partial-differential equation (see references [25, 28, 106, 108])

$$\frac{\partial P(S, t)}{\partial t} = -\mu \frac{\partial [SP(S, t)]}{\partial S} + \frac{\sigma^2}{2} \frac{\partial^2 [S^2 P(S, t)]}{\partial S^2} \quad (15)$$

with the δ -function-like initial condition, $P(S(0), t = 0) = \delta(S(0) - S_0)$. The averaging procedure (13) yields

$$\langle S(t) \rangle = S_0 e^{\mu t} \quad \text{and} \quad \langle S^2(t) \rangle = S_0^2 e^{\sigma_\mu^2 t}. \quad (16)$$

For brevity, we use hereafter the following definition

$$\sigma_\mu^2 = 2\mu + \sigma^2. \quad (17)$$

The variance of GBM is given by

$$\left\langle [S(t) - \langle S(t) \rangle]^2 \right\rangle = S_0^2 e^{2\mu t} \left(e^{\sigma^2 t} - 1 \right). \quad (18)$$

⁸ The log-normal distribution of stock prices after any time interval is another fundamental postulate of the BSM model. The other assumptions are, i.a., (on the ‘model’ level) that trading is continuous in time, the price variations are continuous and jump-free in time, the adjustment to a new information is instant and memory-less, and the actual price reflects all information available. Additionally (on the ‘executorial’ level), no restrictions on short-term sells are imposed, no taxes or retail commissions are to be paid from possible profits, no general transaction/trading fees exist, etc (see reference [25] for option-pricing models with discontinuous price variations). Importantly, for GBM models the volatility is known parameter constant in time, that is a rather unrealistic assumption [120].

For GBM, the exponential growth of $\langle S^2(t) \rangle$ in (16) stems from the BM of the log(price), with the variance of fluctuations growing linearly with time (as in the original Bachelier’s study [1]).

3.2. TAMSD of GBM: nonaged, aged, and delayed cases

The relations (16) and (18) follow from the general ‘stochastic’ solution (11) and one- and two-point probability-density functions of the Wiener process,

$$P_1(W_1, t_1) = \exp\left(-\frac{W_1(t_1)^2}{2t_1}\right) / \sqrt{2\pi t_1} \tag{19}$$

and (at $t_1 > t_2$)

$$P_{12}(W_1, t_1; W_2, t_2) = \frac{\exp\left(-\frac{(W_1(t_1)-W_2(t_2))^2}{2(t_1-t_2)}\right)}{\sqrt{2\pi(t_1-t_2)}}, \tag{20}$$

computing, respectively,

$$\langle S^q(t) \rangle = \int_{-\infty}^{\infty} [S(W, t)]^q P_1(W, t) dW \tag{21}$$

and

$$\langle (S(t) - \langle S(t) \rangle)^2 \rangle = \int_{-\infty}^{\infty} (S(W, t) - \langle S(W, t) \rangle)^2 \times P_1(W(t), t) dW. \tag{22}$$

Similarly, the integrand of TAMSD (1) can be expressed via

$$\begin{aligned} \langle [S(t + \Delta) - S(t)]^2 \rangle &= \int_{-\infty}^{\infty} S^2(W_1, t) \times P_1(W_1, t) dW_1 + \int_{-\infty}^{\infty} S^2(W_2, t + \Delta) \times P_1(W_2, t + \Delta) dW_2 \\ &\quad - 2 \int_{-\infty}^{\infty} \int_{-\infty}^{\infty} S(W_1, t) \times P_1(W_1, t) S(W_2, t + \Delta) \times P_{12}(W_1, t; W_2, t + \Delta) dW_1 dW_2 \end{aligned} \tag{23}$$

that yields

$$\langle [S(t + \Delta) - S(t)]^2 \rangle = S_0^2 \left(1 - 2 e^{\Delta\mu} + e^{\sigma_\mu^2 \Delta}\right) \times e^{\sigma_\mu^2 t}. \tag{24}$$

Taking the final TAMSD integral over t from the last exponent in (24), one gets for the standard (nonaged), aged, and delayed TAMSDs of GBM, respectively,

$$\langle \overline{\delta^2(\Delta)} \rangle = \frac{S_0^2 \left(1 - 2 e^{\Delta\mu} + e^{\sigma_\mu^2 \Delta}\right)}{(T - \Delta)\sigma_\mu^2} \left[e^{\sigma_\mu^2(T-\Delta)} - 1 \right], \tag{25}$$

$$\langle \overline{\delta_a^2(\Delta)} \rangle = \frac{S_0^2 \left(1 - 2 e^{\Delta\mu} + e^{\sigma_\mu^2 \Delta}\right)}{(T - \Delta)\sigma_\mu^2} \left[e^{\sigma_\mu^2(t_a+T-\Delta)} - e^{\sigma_\mu^2 t_a} \right], \tag{26}$$

and

$$\langle \overline{\delta_d^2(\Delta)} \rangle = \frac{S_0^2 \left(1 - 2 e^{\Delta\mu} + e^{\sigma_\mu^2 \Delta}\right)}{(T - \Delta - t_d)\sigma_\mu^2} \left[e^{\sigma_\mu^2(T-\Delta)} - e^{\sigma_\mu^2 t_d} \right]. \tag{27}$$

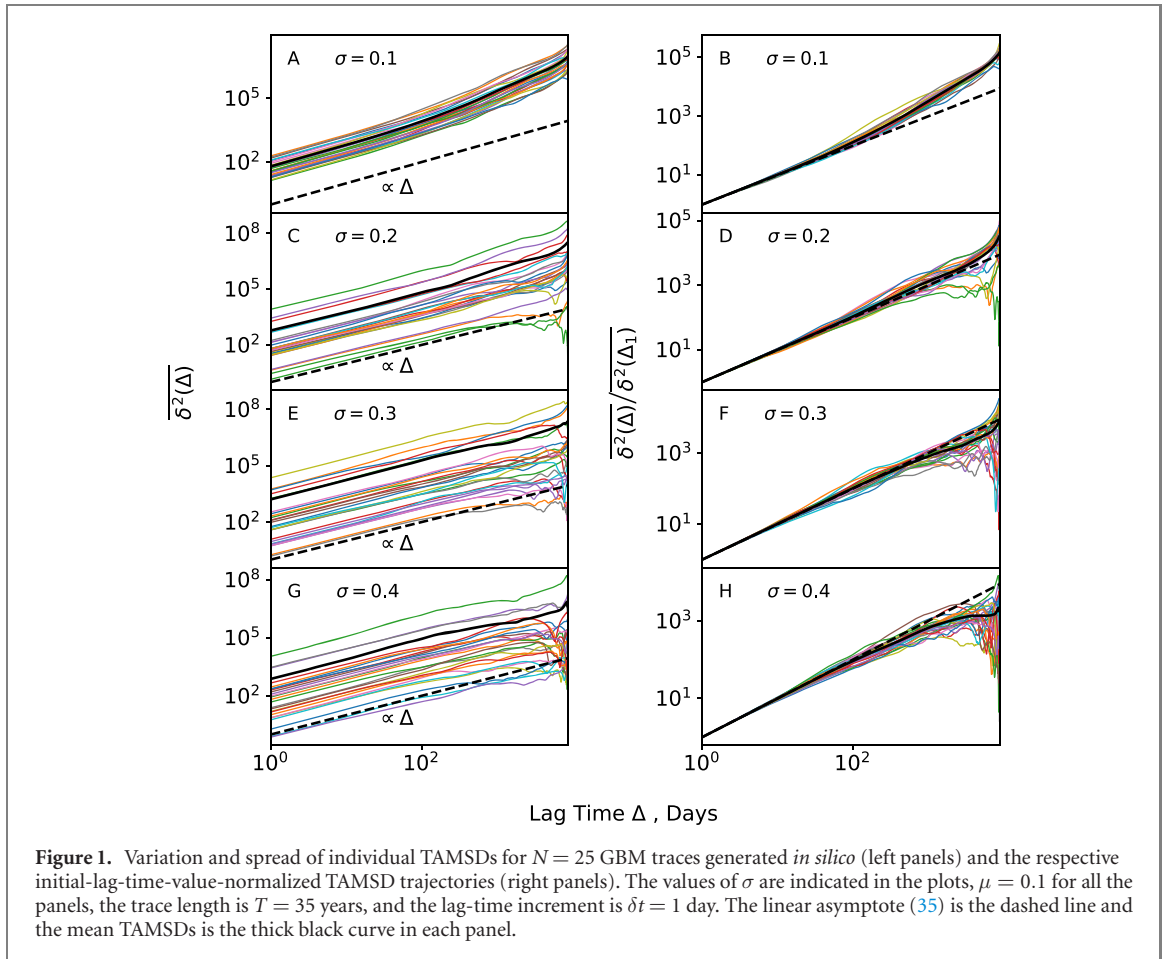
From equation (25) in the absence of drift, at short lag times ($\Delta \ll T$) and for long traces ($\sigma^2 T \gg 1$) one gets the fundamental relation (3) [150]. From equation (26) relation (6) follows at short lag and aging times, $\{t_a, \Delta\} \ll T$. Finally, from (27) at short lag and delay times ($\{t_d, \Delta\} \ll T$) one arrives at the fundamental law (7). The TAMSD analytical expressions (25)–(27) is our **first key result**. Although derived to get the short-time asymptotes before [150], the complete expressions are presented here for the first time. We refer to appendix B for an alternative TAMSD derivation.

4. GBM: results of computer simulations versus theory

4.1. Numerical integration scheme

As follows from (12), to simulate GBM the Wiener process $W(t)$ needs to be exponentiated. The increments of $W(t)$ are independent and normally distributed random variables with mean zero and variance $(t_1 - t_2)$, so that

$$W(t_1) - W(t_2) \sim \mathcal{N}(0, t_1 - t_2). \tag{28}$$



As $W(t_1) \sim \mathcal{N}(0, t_1)$ for $t_2 = 0$, using (12) for the mean and variance of $X(t)$ we get, respectively, $\langle X(t) \rangle = (\mu - \sigma^2/2)t$ and

$$\langle [X(t) - \langle X(t) \rangle]^2 \rangle = \sigma^2 t. \quad (29)$$

The subsequent values of the Wiener process are generated using

$$W_{n+1} = W_n + \sqrt{t_{n+1} - t_n} \times Z_n, \quad (30)$$

where $n = \{0, 1, 2, \dots, \bar{N} - 1\}$ is the discretization index and $Z \sim \mathcal{N}(0, 1)$ obeys the normal distribution for the time points

$$0 = t_0 < t_1 < \dots < t_{\bar{N}} = T. \quad (31)$$

For a stochastic process $X(t)$ defined by (12) using expression (30) we get

$$X_{n+1} = X_n + (\mu - \sigma^2/2)(t_{n+1} - t_n) + \sigma \sqrt{t_{n+1} - t_n} \times Z_n. \quad (32)$$

On the equidistant time-grid with the step-size $\delta t = t_{n+1} - t_n$ the simple recursion formula [33] for GBM then becomes

$$S_{n+1} = S_n \times e^{(\mu - \sigma^2/2) \times \delta t + \sigma \sqrt{\delta t} \times Z_n}. \quad (33)$$

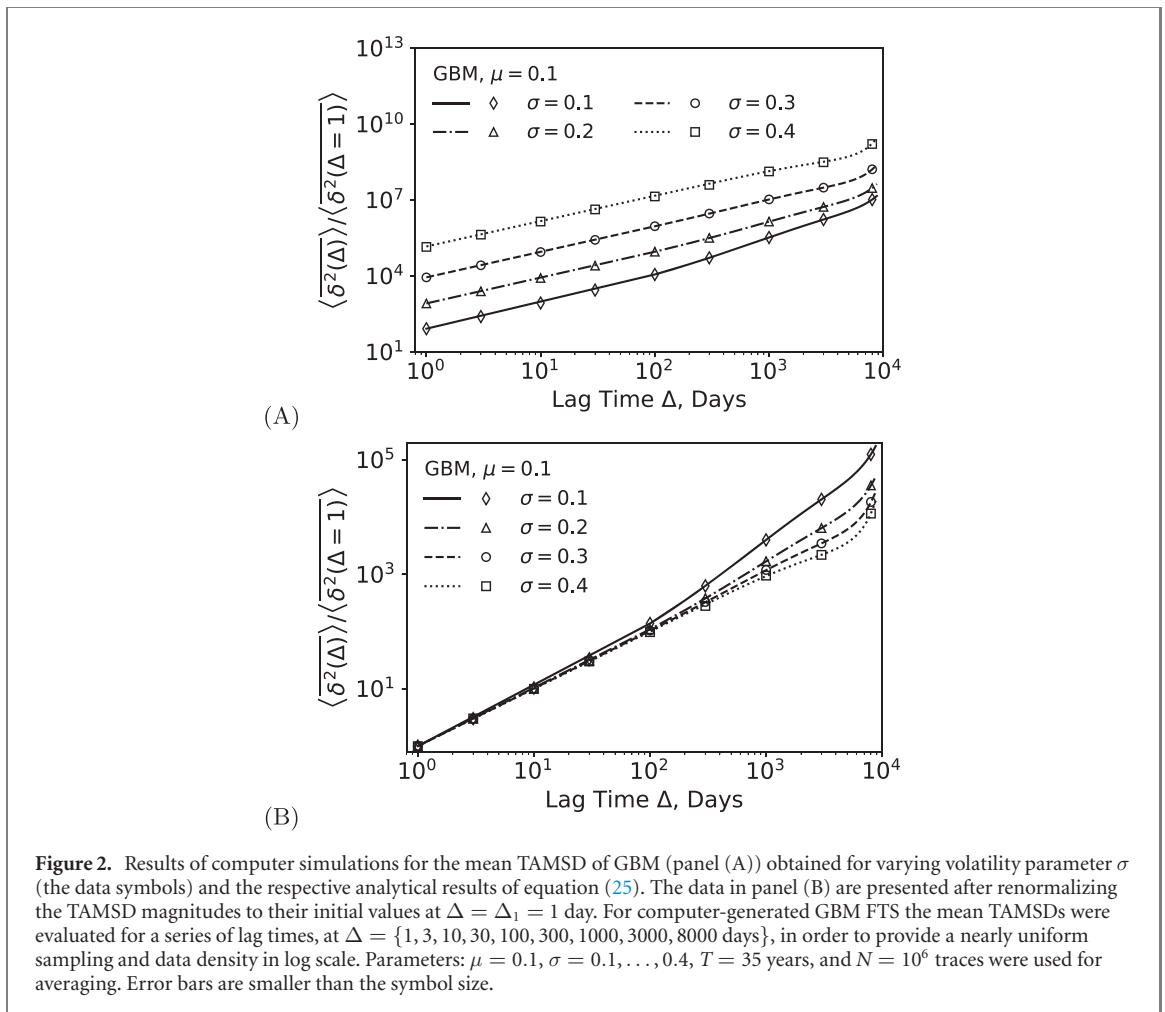
From equation (11) follows that ratio $S(t)/S_0$ is distributed log-normally, namely

$$S(t)/S_0 \sim \log(\mathcal{N}[(\mu - \sigma^2/2)t, \sigma^2 t]), \quad (34)$$

see equation (14). We checked that computer simulations (see figure 1) indeed produce the correct distribution (34), figure AA1. The time-step in the simulations δt was chosen to be 1 business day or 1/252 of the fiscal year (unless explicitly specified otherwise). This makes the results of our simulations straightforwardly comparable with the findings of the analysis of real FTS for classical stocks examined with the same time-step in section 5.1.

4.2. TAMSD

Extensive GBM-based computer simulations deliver novel features for the current study, as compared to the original data-focused study [150]. Some individual *in-silico*-generated GBM trajectories and the respective



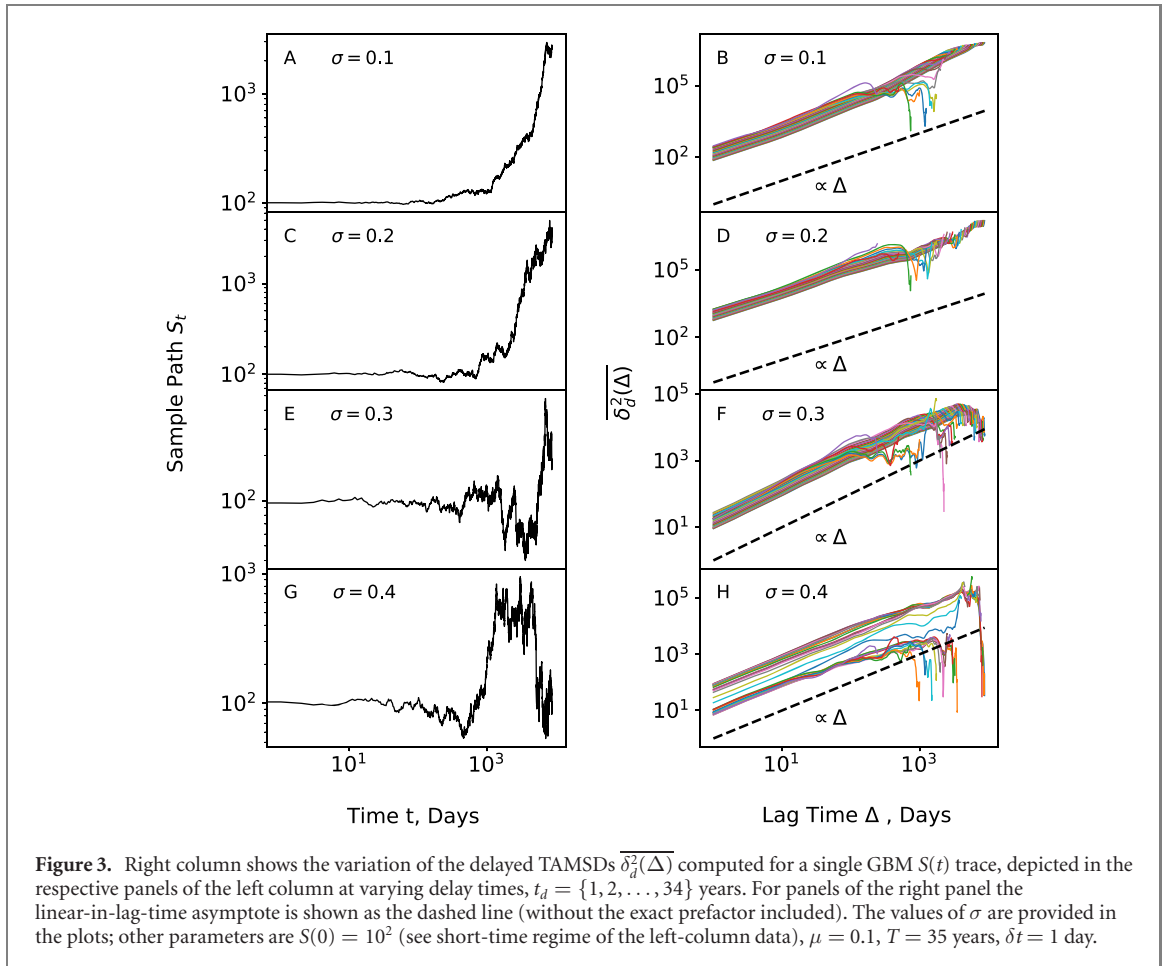
TAMSD paths are shown in figure AA2 for varying trace lengths, $T = \{1, 2, \dots, 35\}$ years. We find that—for the entire range of values of parameters μ and σ used—the TAMSD of GBM for short-to-intermediate lag times the TAMSD of GBM follows a nearly linear scaling with the lag time,

$$\overline{\delta_i^2(\Delta)} \propto \Delta. \quad (35)$$

For longer lag times, a faster growth of the TAMSD and faster-than-linear scaling with the lag time are often observed. In this later region—due to the worsening statistics inherent for the TAMSD definition (1) [154, 155]—considerably fewer increment values are available for time averaging and, therefore, the observed variations of $\overline{\delta_i^2(\Delta)}$ with Δ are much stronger. We mention that for a steadily increasing $S_i(t)$ realization of GBM in simulations the TAMSD magnitude increases for longer trace lengths T , while for stalling or dropping price realizations $S_i(t)$ the TAMSD loses this systematic trend, compare, e.g., figures AA2(B) and AA2(H).

In figure 1 we show $N = 25$ different TAMSD realizations for GBM—each set generated at the same magnitudes of drift and volatility—as functions of the lag time and for the trace length of $T = 35$ years. We recognize the linear scaling of the TAMSD in the region $\Delta \ll T$, equation (35). We also find that for relatively small σ —when the dynamics is mainly impacted by a nonzero value of the drift parameter μ (responsible for the exponential growth of the first moment of GBM, equation (16))—the TAMSDs reveal a faster-than-linear growth at later lag times. The spread of individual TAMSDs in a given set of generated curves decreases for progressively smaller σ values, as expected for the situation when the influence of ‘randomness’ or the underlying volatility of the process decreases, see figures 1(A) and (B).

For larger σ values the reproducibility of TAMSD realizations for GBM naturally decreases: each TAMSD becomes more volatile in magnitude and as a result their spread around the mean value increases dramatically, see figure 1(G). The mean TAMSDs are strongly shifted toward the top region of the distribution of individual TAMSDs, as illustrated in figure 1(G): we find that often a single trajectory with an extremely large magnitude dominates the mean TAMSD. With increasing σ the distributions of TAMSDs in figure 1 reveal larger spreads, typical for the GBM process with higher volatilities.



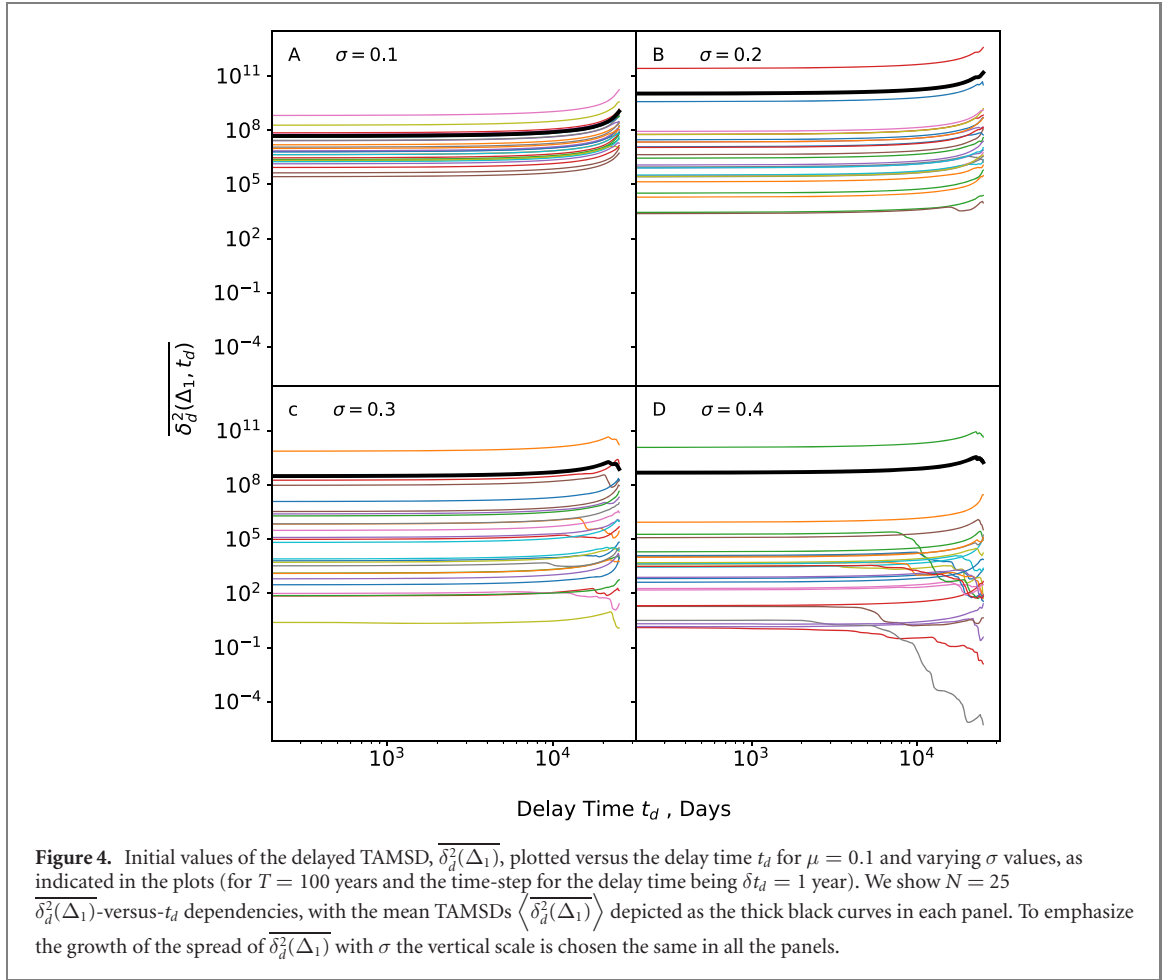
Figures 2(A) and (B) illustrate our **second key result** via demonstrating excellent agreement of the analytical theory for the nonaged mean TAMSD of GBM (25) and the results of computer simulations. The linear scaling of the mean TAMSD with the lag time in the limit $\Delta \ll T$ (shown for some GBM traces also in figures AA2 and 1) is clearly present after averaging. Note that a large set of $N = 10^6$ independent GBM trajectories was used for averaging here, and in most plots with the results of simulations. This very large statistical ensemble is necessary to compensate for outliers and large-deviation trajectories for this multiplicative and innately highly varying GBM process (such a trace is capable of biasing the mean TAMSD for the entire ensemble). The size of a proper averaging ensemble was argued to increase exponentially [197] with the number of points in the time series, \bar{N} , for such processes.

We observe that with increasing volatility σ the magnitude of the TAMSD dramatically increases, see figure 2(A) for the $\langle \overline{\delta^2(\Delta)} \rangle$ variation for GBM. The behavior of the normalized TAMSD, namely of $\langle \overline{\delta^2(\Delta)} \rangle / \langle \overline{\delta^2(\Delta_1)} \rangle$, shown in figure 2(B) reveals that for smaller σ values the faster-than-linear scaling of $\langle \overline{\delta^2(\Delta)} \rangle / \langle \overline{\delta^2(\Delta_1)} \rangle$ with Δ appears earlier, at lag times $\Delta \approx 10^2$ days. For larger volatility values, at $\sigma = 0.3$ and 0.4, we (on the contrary) observe a linear growth of $\langle \overline{\delta^2(\Delta)} \rangle / \langle \overline{\delta^2(\Delta_1)} \rangle$ at intermediate lag times and a highly accelerated growth at later stages, at $\Delta \rightarrow T$. These features are fully consistent with the analytical GBM-based predictions (25) in all regions of the lag time, see figure 2(B).

4.3. Delayed TAMSD

The behavior of individual realizations $\overline{\delta_d^2(\Delta)}$ —computed for a *single* GBM trace for varying delay times t_d —versus the lag time Δ is shown in the right column of figure 3. A key property of the delayed TAMSD [150] is that the later parts of the FTS contribute progressively stronger at longer delay times. We find that, similar to the trends of the standard TAMSD shown in figure 1(G), the variation of the magnitudes of $\overline{\delta_d^2(\Delta)}$ increases for larger volatilities, see figure 3(H).

The variation of the delayed TAMSD computed at the shortest lag time, $\overline{\delta_d^2(\Delta_1)}$, with delay time t_d is shown in figure 4. We focus on the shortest lag time because the magnitudes of the standard and delayed TAMSDs are statistically most reliable at $\Delta/T \ll 1$ [150, 155]. Here we find, as expected, also a wider spread of individual



$\overline{\delta_d^2(\Delta_1)}$ for larger σ values (due to higher variances and larger fluctuations of the GBM process realized for larger volatility values). For larger σ values—as the ‘effective drift’ in the GBM solution (11), given by

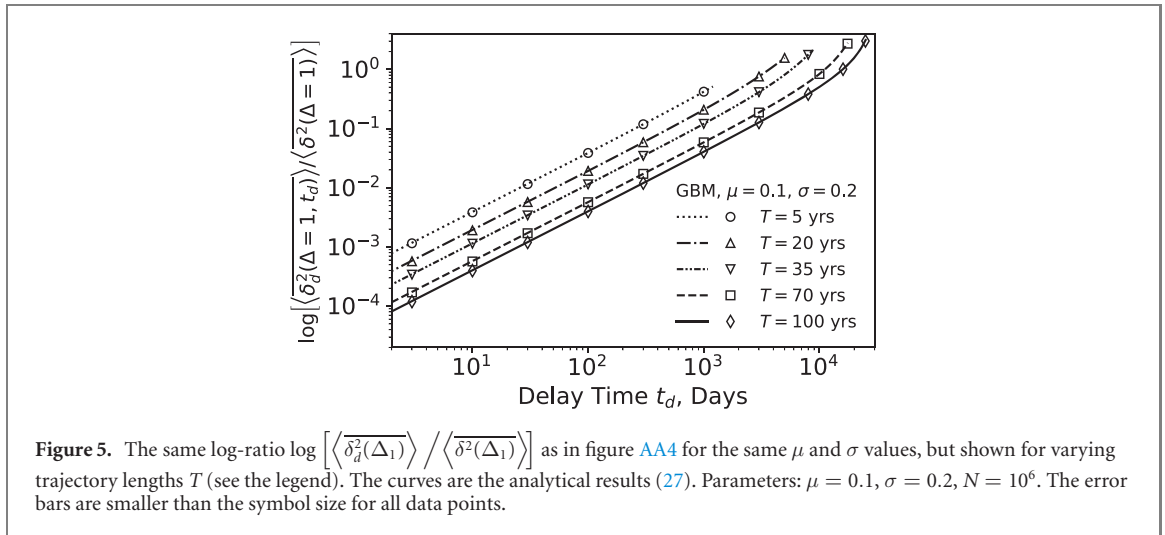
$$\mu_{\sigma,\text{eff}} = \mu - \sigma^2/2, \quad (36)$$

becomes negative—the fluctuations of the Wiener process cannot ensure any sustainable (exponential) price growth for the resulting stochastic process. For this situation, a finite fraction of GBM traces predict drastically *falling* prices $S(t)$ at longer times, a feature of a collapse or bankruptcy, see figure 4(D). In economics, $\mu_{\sigma,\text{eff}}$ is often called the expected growth rate [112]. The mean value $\langle \overline{\delta_d^2(\Delta)} \rangle$ is, however, again often dominated by a single large-magnitude trajectory and, thus, only weakly affected by such price drops observed for some strongly volatile GBM trajectories.

At even larger values of σ used in simulations we find extremely volatile behavior of the resulting $S(t)$ and of the respective $\overline{\delta_d^2(\Delta)}$ realizations. This fact, in turn, gives rise to large variations of $\overline{\delta_d^2(\Delta_1)}$ versus the delay time and, ultimately, to irregularities in the behavior of the mean $\langle \overline{\delta_d^2(\Delta_1)} \rangle$ versus t_d (not shown).

In general, we find that $\langle \overline{\delta_d^2(\Delta_1)} \rangle$ -dependence versus t_d evaluated for different σ values mainly differs in magnitude, while keeping the overall functional form of variation with the delay time, figure AA3. Specifically, $\langle \overline{\delta_d^2(\Delta_1)} \rangle$ reveals almost no variation for short-to-intermediate delay times and exhibits a significant increase of the magnitude at $t_d \rightarrow T$, see figure AA3. The agreement of analytical predictions of equation (27) with the results of computer simulations for $\langle \overline{\delta_d^2(\Delta_1)} \rangle$ is excellent for small-to-moderate volatility values.

For an ensemble of $N = 10^6$ GBM trajectories used for averaging, only the data for the largest μ and σ values are considerably lower than the analytical predictions. We ‘scale’ the results of simulations and shift them up in magnitude for such situations in order to reach the theoretical asymptote. Figure AA3 shows both the original and ‘scaled’ results of simulations for $\langle \overline{\delta_d^2(\Delta_1)} \rangle$. One can argue that for strongly volatile realizations of GBM at large σ values the magnitude of the mean delayed TAMSD can be influenced by a single extreme-magnitude trajectory (see figure 4(D) for an example) that dominates the mean $\langle \overline{\delta_d^2(\Delta_1)} \rangle$. Even larger ensembles of



GBM traces could be required to encounter such large-magnitude trajectories in simulations and to mitigate the observed disparity of theory-versus-simulations in the magnitude of $\langle \delta_d^2(\Delta_1) \rangle$, as detected at larger σ in figure AA3.

The behavior of the log of the mean delayed TAMSD normalized to the standard TAMSD computed at $\Delta = \Delta_1$, namely $\log \left[\frac{\langle \delta_d^2(\Delta_1) \rangle}{\langle \delta^2(\Delta_1) \rangle} \right]$, the universal quantity introduced in reference [150], is shown in figure AA4. The simulations reveal the linear regime of equation (7) for this log-ratio at $t_d \ll T$, as expected, and also confirm a faster-than-linear growth of $\log \left[\frac{\langle \delta_d^2(\Delta_1) \rangle}{\langle \delta^2(\Delta_1) \rangle} \right]$ at intermediate-to-long delay times. Excellent agreement with the theoretical result (27) is observed in our computer simulations for the log-ratio of the normalized delayed TAMSD in the entire range of delay times, see figure 5. This is our **third key result**.

In figure 5 we present the detailed results for $\log \left[\frac{\langle \delta_d^2(\Delta_1) \rangle}{\langle \delta^2(\Delta_1) \rangle} \right]$ for GBM evaluated as function of the delay time t_d for varying trace lengths T . We find that for longer traces the magnitude of $\log \left[\frac{\langle \delta_d^2(\Delta_1) \rangle}{\langle \delta^2(\Delta_1) \rangle} \right]$ drops and the region with a faster-than-linear scaling becomes more pronounced, extending into a larger domain of delay times, at $t_d \lesssim T$. These two trends for the behavior of the delayed TAMSD are fully supported by our analytical results, equation (27). We also mention that for longer trajectories the variation of μ and σ has a considerably smaller effect on the scaling behavior of the log-ratio $\log \left[\frac{\langle \delta_d^2(\Delta_1) \rangle}{\langle \delta^2(\Delta_1) \rangle} \right]$ computed at short delay time t_d , see figure AA5.

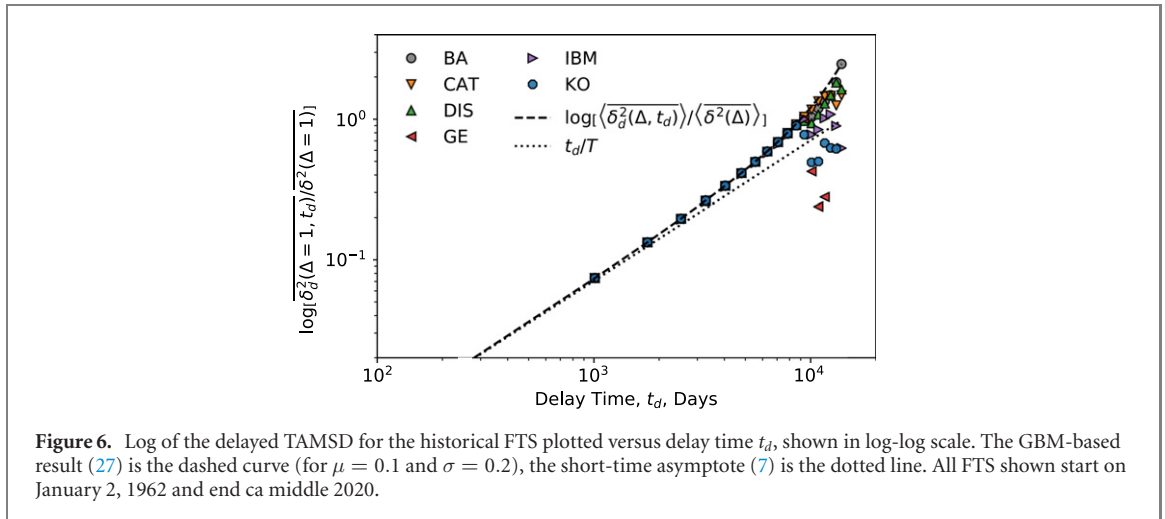
4.4. Ergodicity breaking

Note that the ‘time-rearrangement trick’ (B9) can also be useful [151] for evaluating higher moments of GBM, such as the fourth time-averaged moment that contributes to the ergodicity breaking parameter [154, 155],

$$\text{EB}(\Delta) = \left\langle \left(\overline{\delta^2(\Delta)} \right)^2 \right\rangle / \left\langle \overline{\delta^2(\Delta)} \right\rangle^2 - 1. \quad (37)$$

Computer-generated GBM trajectories reveal a similar scaling for $\left\langle \left(\overline{\delta^2(\Delta)} \right)^2 \right\rangle$ and $\left\langle \overline{\delta^2(\Delta)} \right\rangle^2$ with Δ and, thus, a roughly lag-time-independent value of EB. For trajectory length of $T = 35$ years we find $\text{EB}_{\text{GBM}}(\Delta) \approx 5T/2$, as shown in figure AA6. A detailed analytical study of EB for arbitrary trace length and GBM-model parameters, the simulations-based EB analysis for GBM as well as its applicability to real FTS is the subject of a separate investigation [151].

From simulations we can conclude that GBM is a nonergodic process featuring a finite—rather than vanishing—value of the EB parameter in the limit of long trajectories and short lag times, see figure AA6 at $\Delta/T \ll 1$. Note that the nonergodicity of GBM studied in reference [113] differs in its definition from equation (37). The latter was extensively applied in recent years for assessing weak ergodicity breaking for the *in-silico*-generated trajectories of various stochastic anomalous-diffusion processes [157–164].



5. Analysis of historical FTS

With these theoretical concepts and results (in particular, regarding the $\overline{\delta_{d,i}^2(\Delta)}$), we proceed now to the analysis of historical FTS. For real data we compute the same observables as for the simulated GBM trajectories and examine to what extent the GBM-model predictions are applicable.

5.1. Data acquisition

The acronyms of the companies, stocks and cryptocurrencies analyzed below are, respectively, {BA: Boeing Comp., CAT: Caterpillar Inc., DIS: The Walt Disney Comp., GE: General Electric Comp., IBM: International Business Machines Comp., KO: Coca-Cola Comp., MCD, McDonald's Corporation, S & P 500: Standard & Poor's 500} and {BTC, BitCoin, ETH, Ethereum, LTC, Litecoin}. The data for the companies and cryptocurrencies were downloaded from the Yahoo-Finance web-page (<https://finance.yahoo.com>) with time-step of $\delta t = 1$ day. The data at the end of day-trading sessions are used in the analysis (closure prices)⁹. The corporations chosen feature long FTS (without any rebranding, splitting, merging, etc). The FTS of stock-market indices and cryptocurrencies used in the analysis are presented in figures AA8 and AA9, respectively.

5.2. Universal behavior of the delayed TAMSD

5.2.1. Companies/indices

For the chosen FTS of stock-market prices, the log-ratios of the normalized delayed TAMSDs, $\log \left[\frac{\overline{\delta_d^2(\Delta_1)}}{\overline{\delta^2(\Delta_1)}} \right]$, demonstrate the universal behavior via collapsing onto a *single master curve* as functions of t_d/T , see figure 6. The most pronounced feature is the fact that at short-to-intermediate delay times—in crisis-free times, when the GBM-model itself is applicable—the FTS yield the delayed TAMSD that follows the linear GBM-conform law (7) [150]. The deviation of $\log \left[\frac{\overline{\delta_d^2(\Delta_1)}}{\overline{\delta^2(\Delta_1)}} \right]$ as function of t_d from this law at later delay times FTS is also in excellent agreement with the GBM-based prediction (27)¹⁰. The latter is valid at all values of lag and delay times yielding our **fourth key result**. We stress here that all data points were used in the analysis, without any pre-selection, both for the crisis-containing and crisis-free times.

A severe drop of the delayed TAMSDs at the end of some trajectories in figure 6 is the result of the three latest economic crises; this region with rapidly falling prices is (naturally) in disagreement with GBM predictions. We quantify these deviations below via analyzing the data in log-linear scale, for only later segments of the FTS and for smaller delay-time increments, δt_d . The pronounced deviations from the GBM predictions at later delay times are, naturally, due to the respective *drastic crisis-induced price drops*. In figure 7 we relate the delay

⁹ Note that multiple manipulative instruments are ubiquitously used—such as share repurchase (stock buyback), share splitting [and also reverse stock split], stock dilution, etc.—that lead to “recalibration” of the respective stock prices. The “close” market data (from <https://finance.yahoo.com>) we used are normalized for splits, but not for dividends, repurchases, or dilutions. The exact and specific mechanisms of stock-price increase expected, e.g., after a stock-split event—due to a wider “pool” of interested buyers—which leave, however, the fundamental value of a given company unaffected, are beyond the scope of the current study.

¹⁰ Note that this consistency of stock-price variations and growth with the GBM model for a set of traditional stocks we examined over a period of several decades does not exclude a possibility of bankruptcy of a random stock. Such a scenario is also realizable for a multiplicative process of GBM: once the price of a stock/option hits zero, it stays zero forever.

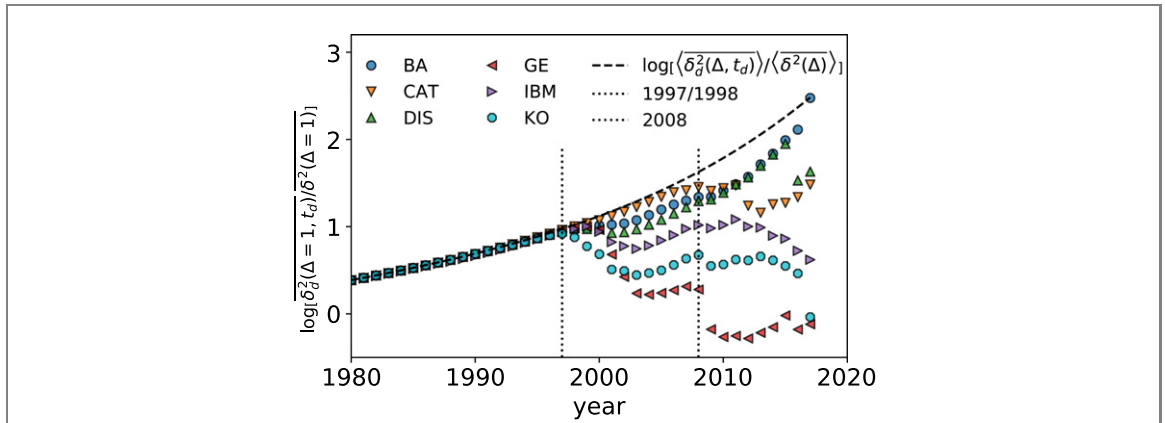


Figure 7. Log of the rescaled delayed TAMSD plotted versus the actual date of FTS, shown in log-linear scale. The GBM-based asymptote (27) is the dashed curve, plotted for $\mu = 0.1$ and $\sigma = 0.2$. The step of the delay time is $\delta t_d = 1$ year (that is about 252 business days per one fiscal year [for classical stocks]). The starting date of the analyzed FTS data is 1962, the results are shown starting from 1980. The economic crises of 1997–1999 and 2008–2009 are indicated by the dotted vertical lines.

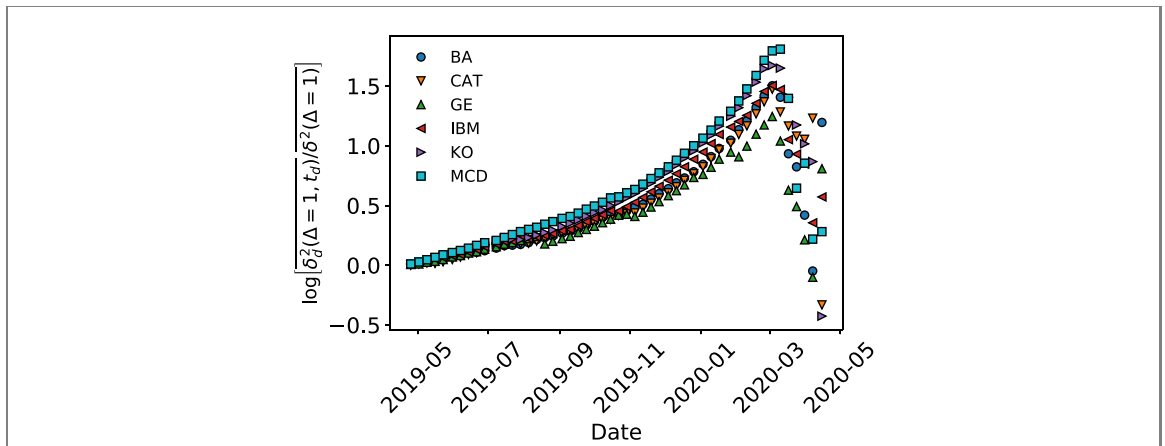
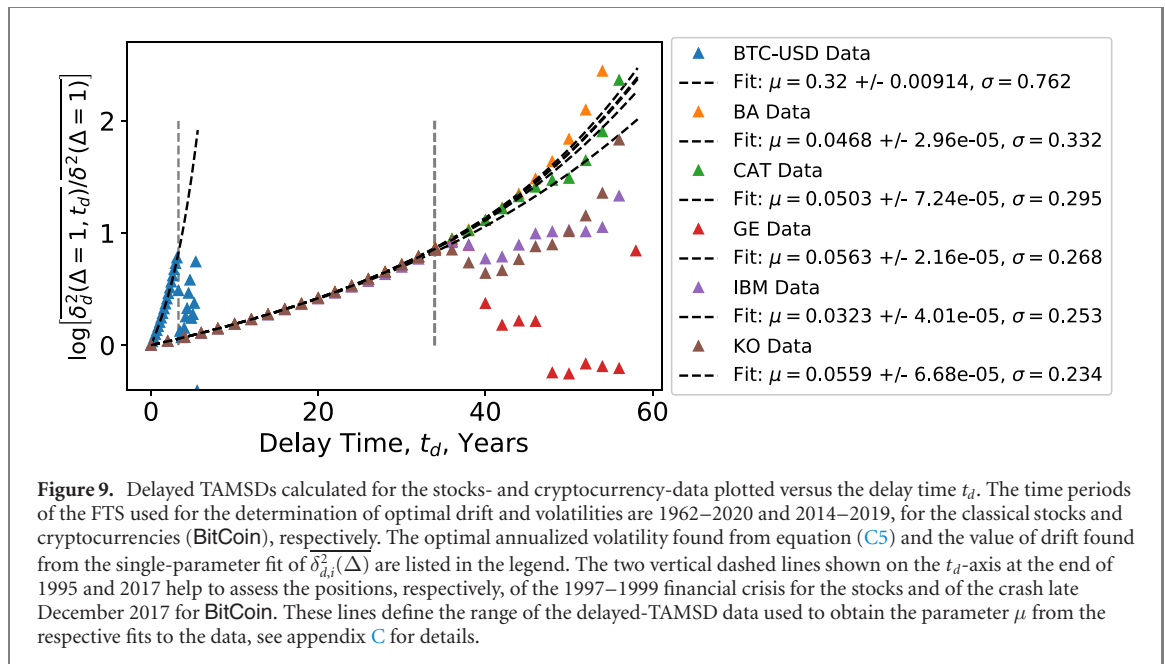


Figure 8. The same as in figure 7, but for the FTS for a period of the last year only, plotted in terms of $\log \left[\frac{\delta_d^2(\Delta_1)}{\delta^2(\Delta_1)} \right]$ versus the actual calendar date (recalculated from the respective t_d values), with the delay-time step of $\delta t_d = 5$ days. The drop in the magnitude at the start of the 2020 economic decline triggered by Covid-19 pandemic is clearly visible from ca March 2020.

times t_d to the actual calendar date of the respective FTS. This way, we relate the time of drops in $\overline{\delta_{d,i}^2(\Delta)}$ to the respective economic perturbations/crisis, compared to plots versus the t_d itself, as in figure 6.

In figure 7 we demonstrate a quantitative agreement with the theoretical GBM-based predictions (27) for the actual historical FTS in crisis-free times. We also find that the drops of $\log \left[\frac{\delta_d^2(\Delta_1)}{\delta^2(\Delta_1)} \right]$ versus t_d indeed corresponds to the periods 1997–1999 and 2008–2009 (the Russian/Asian and financial crises, respectively). The ongoing 2020 world-wide economic decline triggered by the ongoing Covid-19 pandemic is also visible for the later parts of the analyzed FTS, as indicated in figure 8. The latest stock-price variations are particularly well visible and pronounced when the delayed TAMSD data are presented for the last prior-to-crisis months only and with the minimal step of $\delta t_d = 1$ day in order to resolve daily fluctuations (results not shown). Naturally, rapid variations of the log-ratio of the delayed TAMSDs at later parts of FTS are then resolved much better, as compared to the case of $\delta t_d = 1$ year shown in figure 7.

After the 2008–2009 crisis with a partial ‘resetting’ [165, 166] of many stock-market indices to a certain extent we observe that some indices started to continue their (exponential) GBM-like price growth again, thereby reloading the price-explosion spring (results not shown). Note also that choosing the end point of FTS well after the peak of a financial crisis *smears out* the crisis-induced drop of prices when evaluating the TAMSD and reduces the deviations from the GBM $\log \left[\frac{\delta_d^2(\Delta_1)}{\delta^2(\Delta_1)} \right] \sim t_d/T$ asymptote, see equation (7). This happens as typically higher prices occur at later stages in the FTS. This is why *no decrease* is visible, for instance, in the S & P 500 long-time data when plotted in terms of $\log \left[\frac{\delta_d^2(\Delta_1)}{\delta^2(\Delta_1)} \right]$ versus t_d in October 1987, at the time of S & P 500 crash, see figure AA7 (and also the results of reference [150]).



5.2.2. Cryptocurrencies

Some ‘digital’ assets, such as BitCoin and other cryptocurrencies, see figure AA9, are extremely speculative, volatile, and nontransparent [146] in their price-formation strategies. Their FTS can potentially feature super-exponential [147] price evolution in crisis-free times and at ‘bull-market’-conditions. This is a snow-ball-like, heating-up, herd-driven [83] phase of price ‘explosion’ characteristic of financial pyramids (with no ‘real value’ supporting the growth). Our current preliminary analysis of some cryptocurrencies quite surprisingly, however, indicates a good agreement with GBM-like variation for $\delta_{d,i}^2(\Delta)$, see figure 9, but with significantly elevated values of drift and volatility, see appendix C for the detailed description of the data-driven algorithms of determination/extraction of the GBM model parameters.

The dependencies of the trajectory-specific quantifier $\log \left[\frac{\delta_d^2(\Delta_1)}{\delta^2(\Delta_1)} \right]$ for the FTS of the ‘classical’ stocks and of three cryptocurrencies versus the GBM predictions for $\log \left[\frac{\langle \delta_d^2(\Delta_1) \rangle}{\langle \delta^2(\Delta_1) \rangle} \right]$ evaluated for the {drift, volatility} pairs determined from the data are shown in figure 9, both as functions of the delay time t_d . The highly speculative nature of the ‘contemporary’ cryptocurrencies gets reflected in *much larger* respective drift and volatility values, as compared to the ‘classical’ stocks, see figures BB2 and BB3. The direct comparison in terms of the variation of the delayed TAMSD versus the delay time—demonstrates an expected *much steeper* growth of the log-ratio for the cryptocurrencies in the same range of delay times, as visible in figure 9. Despite this, the general trends of the growth of $\delta_{d,i}^2(\Delta)$ with the delay time for the cryptocurrencies are well-described by the standard-GBM theoretical model.

We stress that such a comparison is performed in the *same* range of lag times implies similar time-scales for all the stocks and currencies examined here. The ‘agility’ and also the anticipated ‘life-time’ of a given stock or asset (or a class of those) are, however, inherently specific. Evidently, the market of cryptocurrencies is much more dynamic and speculative than that of ‘classical’ assets/commodities (some of them with a century-long history, such as that of trading and pricing gold). This determines, or at least affects, the characteristic ‘internal’ time-scale and also sets an ‘effective temperature’ that ‘heats up’ the growth and overall dynamics of a given stock or asset, an issue deserving future investigations.

6. Discussion and conclusions

6.1. Summary of the main results

We presented the time-averaging-based analysis of the historical FTS of stock-price evolution. We first compared the analytical GBM-based predictions and reported the results of extensive GBM-based computer simulations. Our main focus was on the behavior of the novel observable, the delayed TAMSD [150]. This single-trajectory quantifier—the term ‘inherited’ from the data analysis in single-particle-tracking experiments—is demonstrated here to reveal a universal behavior for the log-ratio $\log \left[\frac{\delta_d^2(\Delta_1)}{\delta^2(\Delta_1)} \right]$ at the shortest lag time $\Delta = \Delta_1$ as a function of the delay time t_d . This universality in the *entire range of delay times* (in crisis-free times) complements the initial analysis at $t_d \ll T$ in reference [150].

Additionally, our FTS-analysis revealed a transition from a linear to a faster-than-linear growth regime for $\log \left[\overline{\delta_a^2(\Delta_1)} / \overline{\delta^2(\Delta_1)} \right]$ as function of the delay time t_d , in full agreement with GBM-based predictions (in crisis-free times). Certain deviations from this ‘ideal’ GBM-like behavior found for the delayed TAMSD in real FTS were shown to be clearly attributable to market collapse associated with the dramatic price drop during respective financial crises.

One more novel element of the current analysis compared to reference [150] is the procedure of determination and optimization of the GBM-model parameters and direct fit of $\overline{\delta_{d,i}^2(\Delta)}$ versus delay time, as detailed in sections C2 and C3 of appendix C. We compared several methods to extract σ and μ and employed finally the most rational and consistent approach, see the results of figure 9. We found that the historical FTS for the highly speculative BitCoin demonstrated the extreme growth in magnitude of the $\log \left[\overline{\delta_a^2(\Delta_1)} / \overline{\delta^2(\Delta_1)} \right]$ within a few years of delay time t_d . The similar-in-magnitude growth is achieved by the classical stocks only within $\approx 30 \dots 40$ years. This once again indicates a bubble-like nature and lack of sustainability of BitCoin and other cryptocurrencies. This parameter-determination procedure enabled us to fit and quantitatively compare the TAMSDs for individual historical FTS, that is the **fifth key result** of our study.

6.2. Extensions and future developments of GBM-based models

A more detailed analysis, that would potentially include some generalized GBM-based models featuring super-exponential MSD growth,

$$\langle S^2(t) \rangle \sim e^{\sigma_\mu^2 t^\beta}, \quad (38)$$

with $\beta > 1$, a ‘scaled-GBM’ process recently introduced in reference [167]. The nonlinear nature of another type was included in the models with the return rate and volatility growing nonlinearly with the price, such that

$$\sim \sigma S(t)^m dW(t) \quad (39)$$

enters the right-hand side of equation (9) (see equation (24) in reference [139]). This simple nonlinear generalization of GBM accounts for a positive feedback and herding behavior (a price-driven model of speculative bubbles). Certain bursts of volatility accompany the approach to and the transition across the ‘bubble point’ in this kind of models. Anomalous behavior of the markets, particularly with a superexponential price growth [147, 148] at and near the bubble corresponds to $m > 1$ choice in equation (39).

For the standard GBM model, the parameters μ and σ are assumed to have constant values, while in reality they can be complicated functions of time, price, and numerous other factors. Often, the real markets reveal, e.g., an increased volatility when the prices drop [168, 169], nonlinear price-volatility correlations [93, 170], anticorrelations of returns and future volatility values [171], the periods of persistent volatility [172, 173], correlations of the trading volumes and intraday volatility [175], and rich dynamics of (nonstationary) intraday price increments [174, 176]. The effects of ‘volatility clustering’—with large price changes being followed by large ones (and vice versa)—and possible long-term memory in volatility are the general ‘stylized facts’ [177] for some FTS. We refer to references [32, 33, 36, 178] for the models of stochastic volatility and to reference [179] for the analysis of finely and coarsely defined volatilities. This feature is treated, i.e., in the models of generalized autoregressive conditional heteroscedasticity (GARCH) [44, 119, 149, 180–184] and autoregressive moving average (ARMA) (see also references [185, 186] for the integrated, actual, and realized volatility as well as higher moments of volatility [185]; the multifractal analysis of financial markets is presented recently in reference [187]). Large volatilities—peaking at the time of big financial crashes [169]—imply rapid price changes and risky trading [173, 188]. In particular, the future values of volatility of an asset are hard to assess: this leads to often imprecise predictions and necessitates modified BSM models [38, 39, 88, 189] via including, e.g., ‘implied volatility’ concepts [190].

Specifically, the description of the ‘Joseph’, ‘Noah’, and ‘Moses’ effects—accounting, respectively, for long-time correlations (or nonindependence), nonfinite variance (or ‘fat tails’), and time-dependence (or nonstationarity) in the distributions of increments of a stochastic process—for the FTS-analysis was presented in reference [176]. A pronounced nonstationarity of the variance of increments for the daily stock-market prices was also demonstrated [174, 175]. The distinct, U-shape-like, stark volatility variations obtained from the high-frequency-data analysis—shown to be universal for a number of indices and currencies [174, 175], being also positively correlated with the respective trading volumes—are inherent to the intraday volatility and stocks-trading activity. This time-dependent diffusion [174] is vital for understanding the rich and complicated dynamics of daily evolution of stock prices and trading volumes. Particularly high volatilities were also observed at the start of the morning trading sessions [175]. The related effects on longer time scales, with higher returns on Mondays and during the first weeks of January (connected to larger price variations), are also documented [138].

The ‘diffusion coefficient’ or volatility was also shown to depend on time and currency exchange rate, with several intervals during the day when the standard deviation of increments revealed distinct, multiple power-law-like scaling behaviors with time, also featuring drastic variations of the intraday-volatility magnitude [174, 191, 192]. This can give rise to ‘spurious’ [174] non-Gaussianity in the distributions of price increments, including Laplace-like forms [193]. Such non-Gaussian features were ubiquitously observed [194, 195] when averaging over longer time-scales was employed and simple/standard time-independent model parameters were used in the fitting analysis. Note that this complicated but repeatable intraday dynamics of the GBM-model parameters favors ensemble-averaging-based analysis [192, 196]—with a large set of daily trading data composing a statistical ensemble of (independent) realizations,—as compared to the methods of time averaging, such as those employed in the current study. The standard GBM model with constant drift and volatility should, thus, be essentially modified to account, e.g., for a power-law variation of volatility [174, 191, 192], $\sigma(t) \sim t^\gamma$, advocating for a new multiplicative stochastic process of ‘scaled’ GBM [167].

Author contributions

All the authors have made a substantial intellectual contribution to the work and approved it for publication.

Competing interests

The authors have no competing interests to declare.

Acknowledgments

A G C is deeply grateful to Humboldt University of Berlin and to Professor I M Sokolov personally for hospitality and support. A G C thanks V G Cherstvy and S Thapa for their help with some graphs and A Serafimovich for providing reference [198]. A G C thanks H Safdari, J Shin, S Thapa, and W Wang for their long-time help with providing scientific articles inaccessible from University of Potsdam. RM acknowledges financial support by the Deutsche Forschungsgemeinschaft (DFG Grants ME 1535/7-1 and ME 1535/12-1). RM also thanks the Foundation for Polish Science (Fundacja na rzecz Nauki Polskiej) for support within an Alexander von Humboldt Polish Honorary Research Scholarship.

Data availability statement

The data used in this study were accessed from <https://finance.yahoo.com>.

Abbreviations

BM Brownian motion

GBM Geometric BM

FTS Financial time series

BSM model Black–Scholes–Merton model

MSD Mean-squared displacement

TAMSD Time-averaged MSD

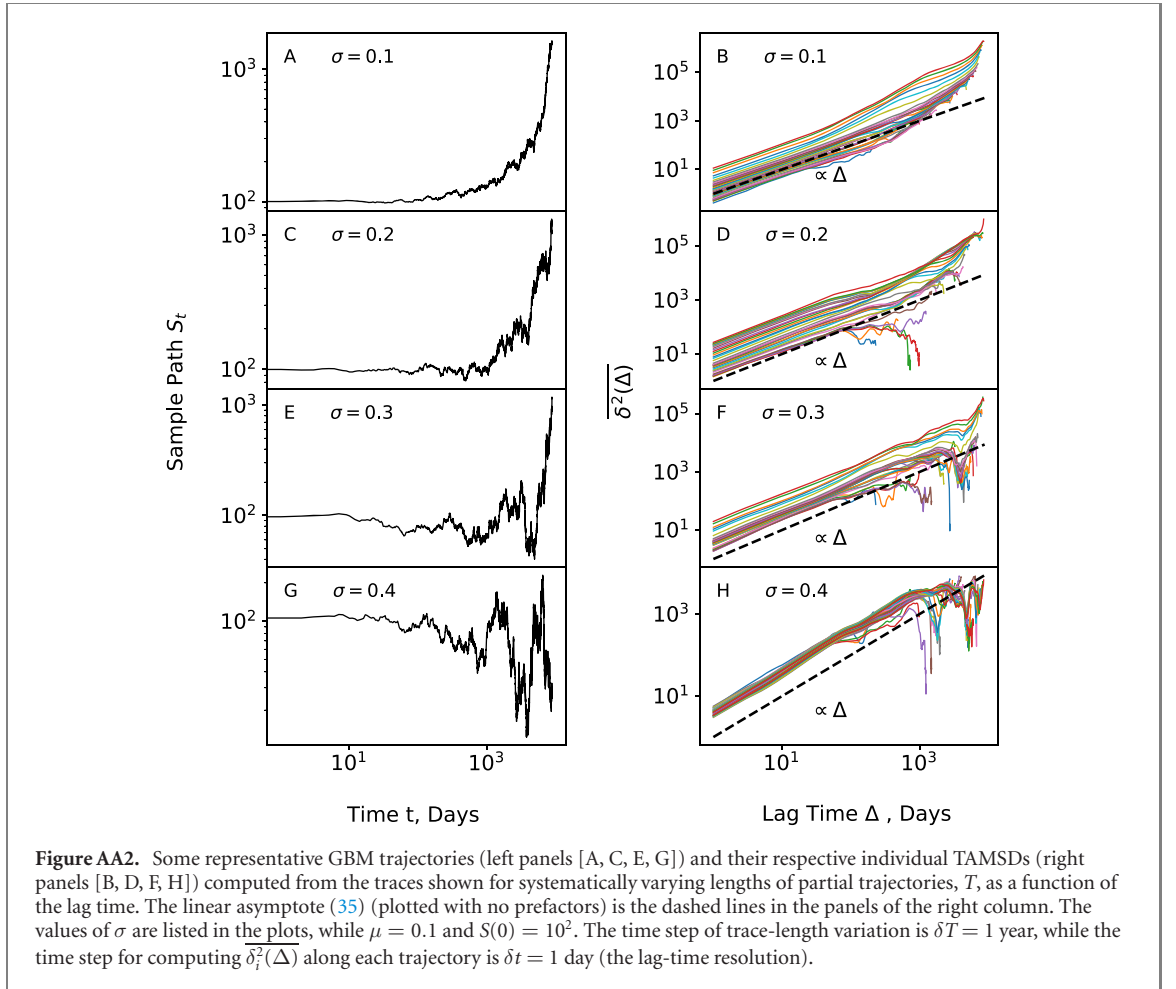
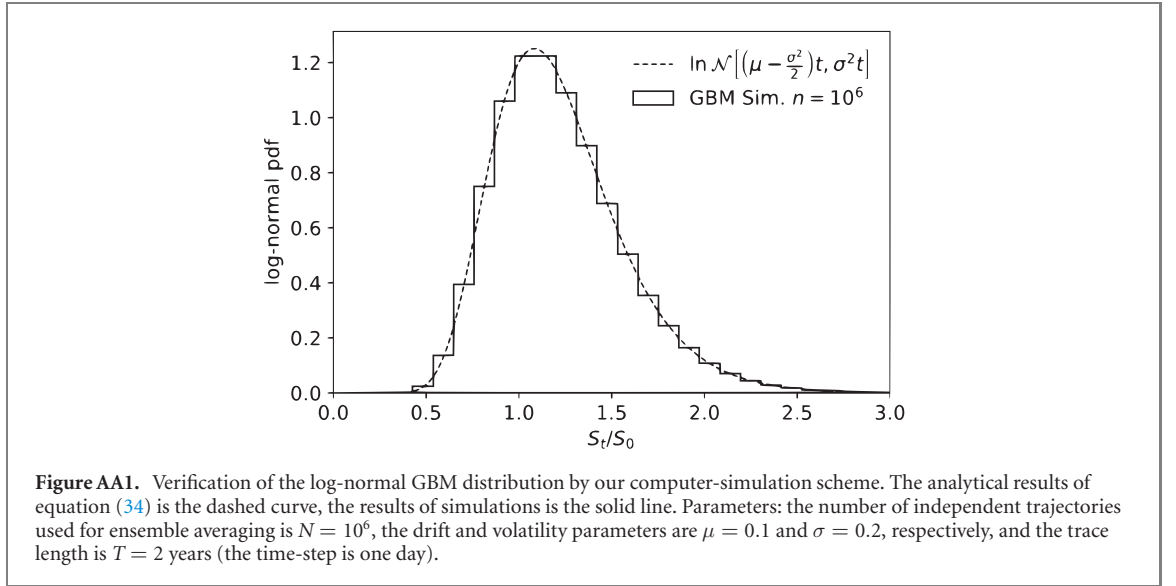
Appendix A. Supplementary figures

Here, we present some auxiliary figures supporting the claims in the main text.

Appendix B. Alternative TAMSD derivation

Expression (25) can also be computed via starting with the integrand in (1) after ensemble averaging,

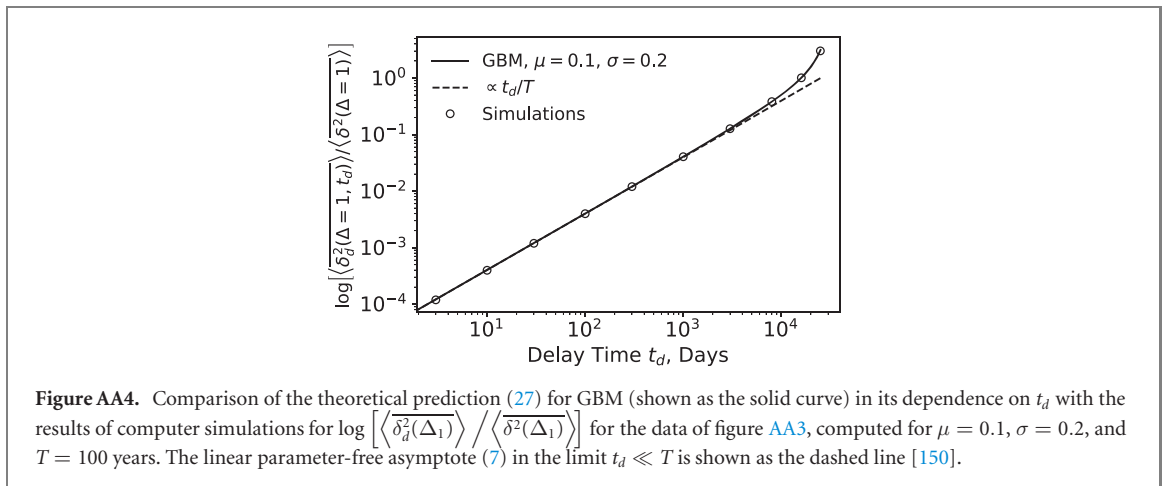
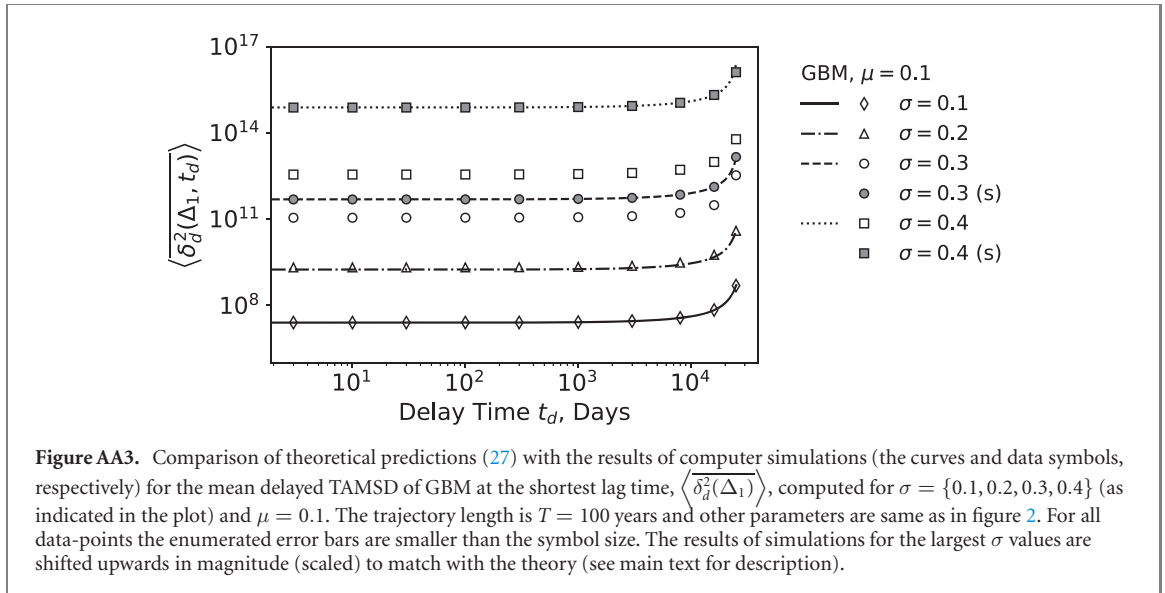
$$\langle [S(t + \Delta) - S(t)]^2 \rangle = \langle S^2(t + \Delta) \rangle - 2 \langle S(t + \Delta)S(t) \rangle + \langle S^2(t) \rangle, \quad (\text{B1})$$



with $S(t)$ following equation (11). The terms without cross-correlations can be computed using that $W(t)$ samples the normal distribution $\mathcal{N}(0, t)$. Using (19), the moment of order $2n$ of $W(t)$ is given by

$$\langle W^{2n}(t) \rangle = 2^n \Gamma(n + 1/2) \pi^{-1/2} \times t^n, \quad (B2)$$

where $\Gamma(x)$ is the gamma function. The first nonzero moments are $\langle W^2(t) \rangle = t$, $\langle W^4(t) \rangle = 3t^2$, $\langle W^6(t) \rangle = 15t^3$, etc. Summing the terms in the Taylor expansion



$$\langle e^{\sigma W(t)} \rangle = 1 + \left(\frac{1}{2} \sigma^2 t \right) + \frac{1}{2} \left(\frac{1}{2} \sigma^2 t \right)^2 + \frac{1}{6} \left(\frac{1}{2} \sigma^2 t \right)^3 + \dots \quad (B3)$$

we get

$$\langle e^{\sigma W(t)} \rangle = e^{\left(\frac{1}{2} \sigma^2 t \right)}. \quad (B4)$$

Clearly, equation (B4) also follows from

$$\langle e^{\sigma W(t)} \rangle = \int_{-\infty}^{\infty} e^{\sigma W(t)} P_1(W(t), t) dW(t) = e^{\left(\frac{1}{2} \sigma^2 t \right)}. \quad (B5)$$

This yields the second moment of GBM as

$$\langle S^2(t) \rangle = S_0^2 e^{(2\mu - \sigma^2)t} \langle e^{2\sigma W(t)} \rangle = S_0^2 e^{(2\mu + \sigma^2)t}, \quad (B6)$$

with the time-shifted moment being

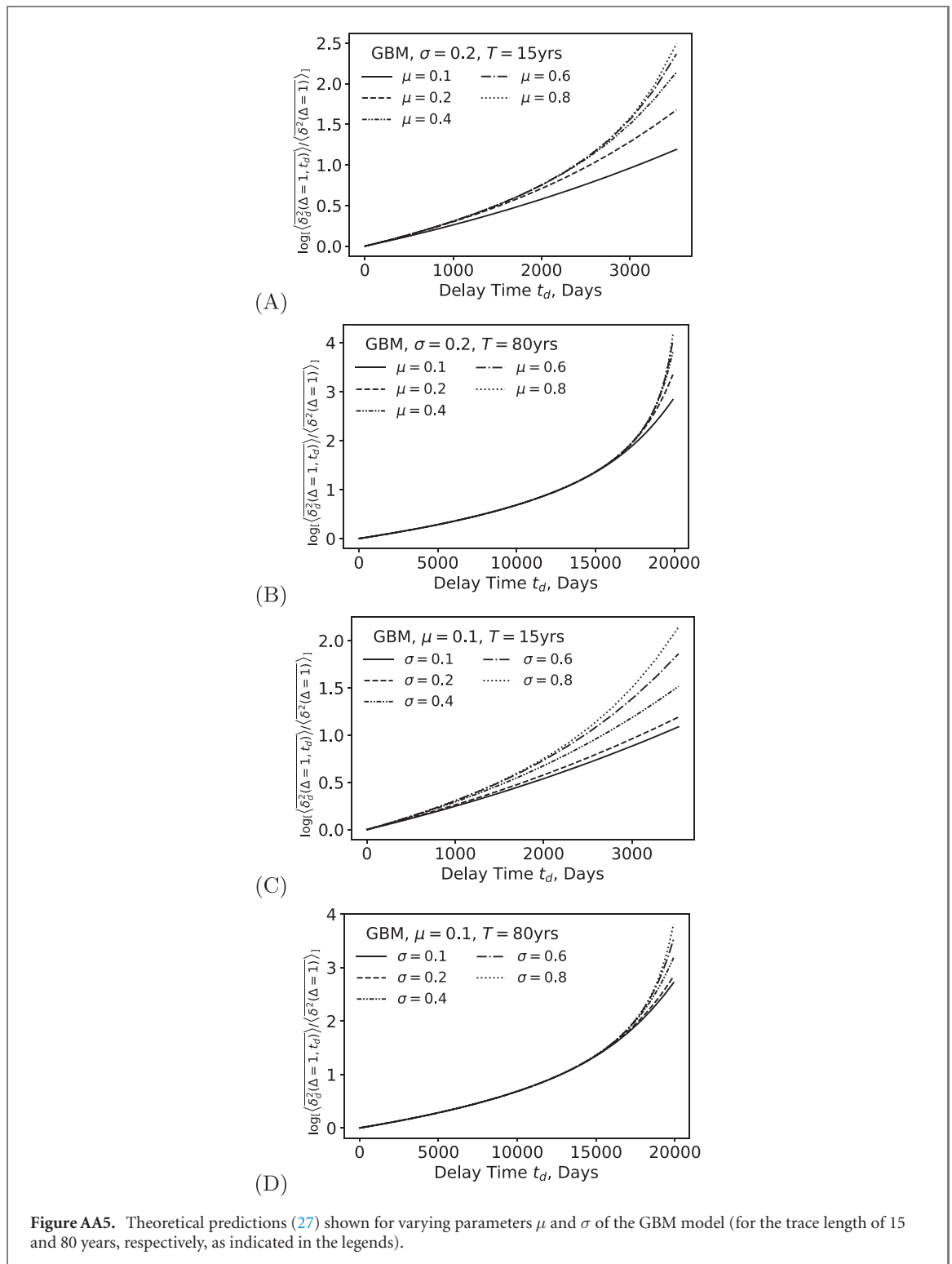
$$\langle S^2(t + \Delta) \rangle = S_0^2 e^{\sigma_\mu^2(t + \Delta)}. \quad (B7)$$

Following the same strategy, for the mixed term in (B1) describing cross-correlations of $S(t)$ and $S(t + \Delta)$ we get

$$\langle S(t + \Delta) S(t) \rangle = S_0^2 e^{2\left(\mu - \frac{\sigma^2}{2} \right)t} e^{\left(\mu - \frac{\sigma^2}{2} \right)\Delta} \langle e^{\sigma(W(t) + W(t + \Delta))} \rangle. \quad (B8)$$

Adding $\sigma(W(t) - W(t))$ to the last exponent in (B8) and using the independence of increments of respective Wiener processes for nonoverlapping time intervals, we arrive at

$$\langle e^{\sigma(W(t) + W(t + \Delta))} \rangle = \langle e^{\sigma(W(t + \Delta) - W(t))} \rangle \langle e^{2\sigma W(t)} \rangle. \quad (B9)$$

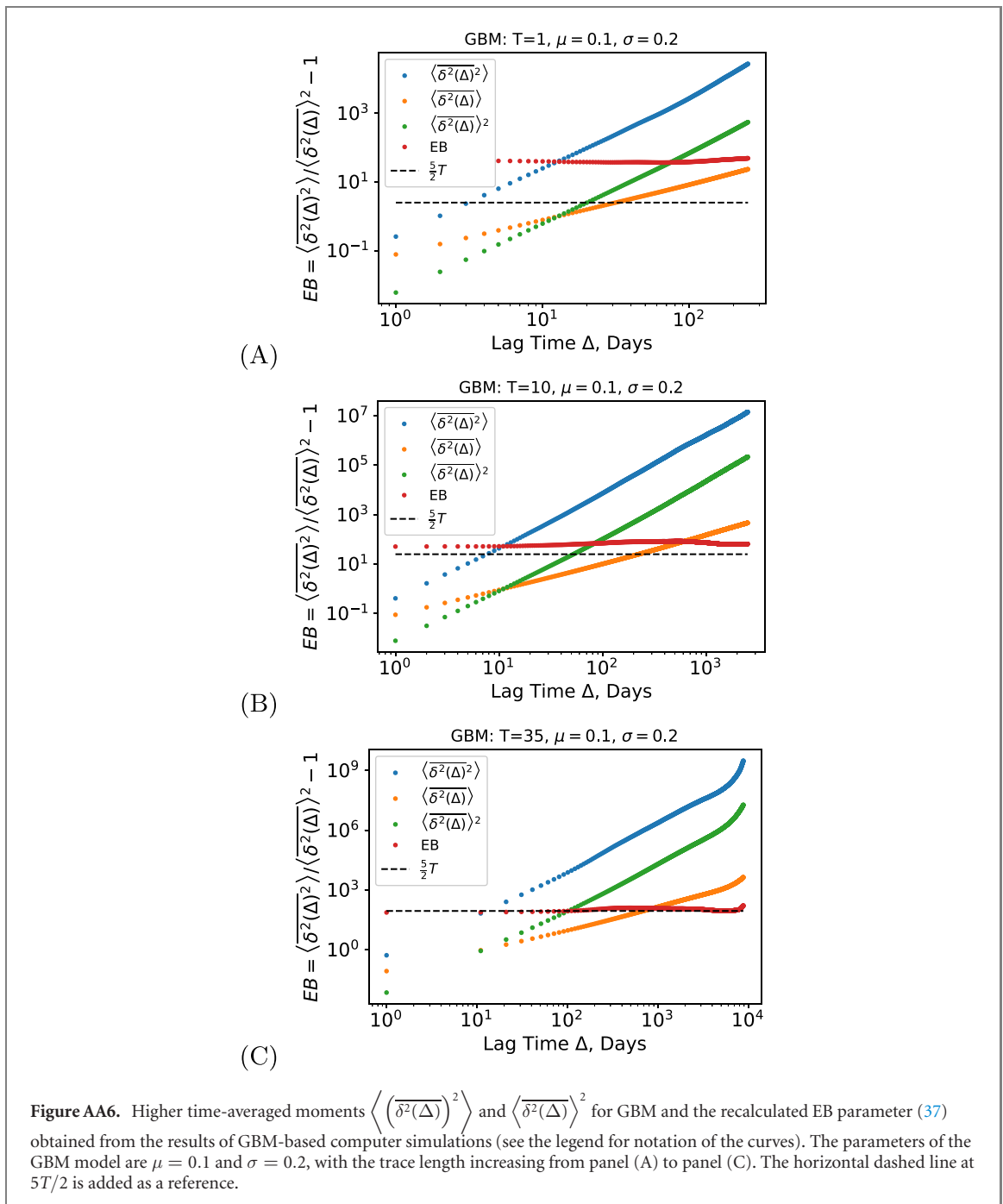


Using (B4) and the distribution of increments $W(t + \Delta) - W(t) \sim \mathcal{N}(0, \Delta)$ (another independent variable), we get

$$\langle S(t)S(t + \Delta) \rangle = S_0^2 e^{\sigma_\mu^2 t + \mu \Delta}. \tag{B10}$$

Thus, for the TAMSD integrand of GBM—putting together (B6), (B7), and (B10)—we arrive at the same expression (24),

$$\langle [S(t + \Delta) - S(t)]^2 \rangle = S_0^2 \left(e^{\sigma_\mu^2 \Delta} - 2e^{\mu \Delta} + 1 \right) e^{\sigma_\mu^2 t}. \tag{B11}$$



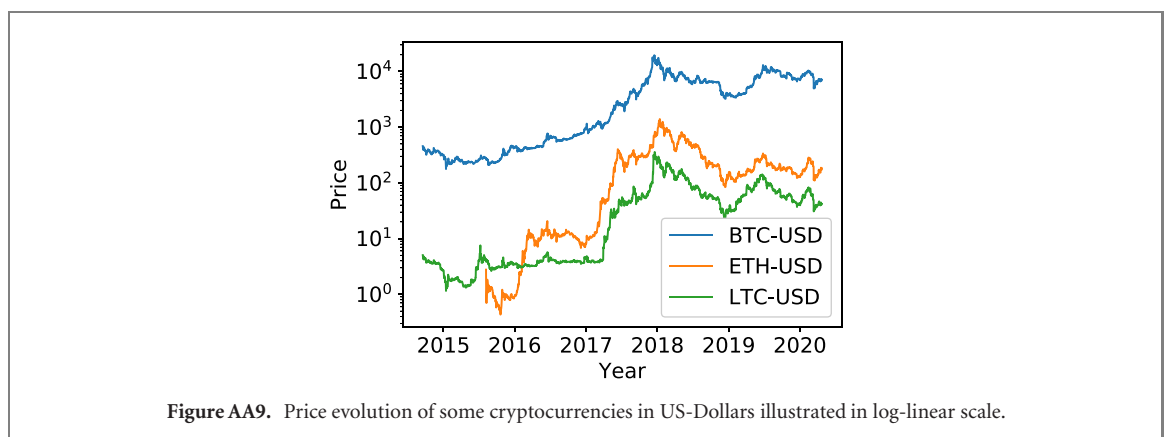
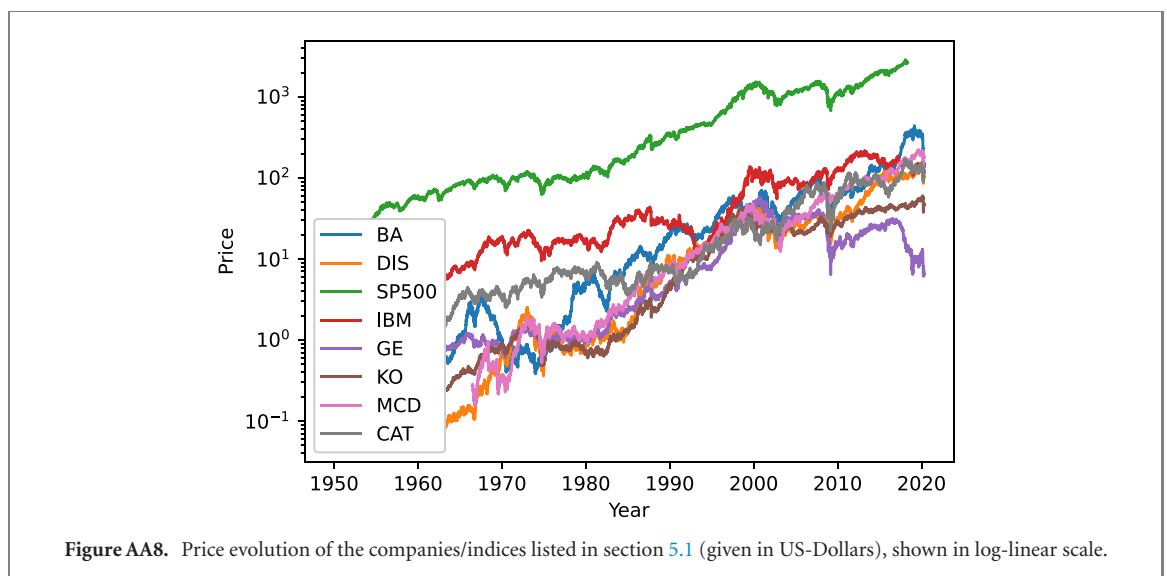
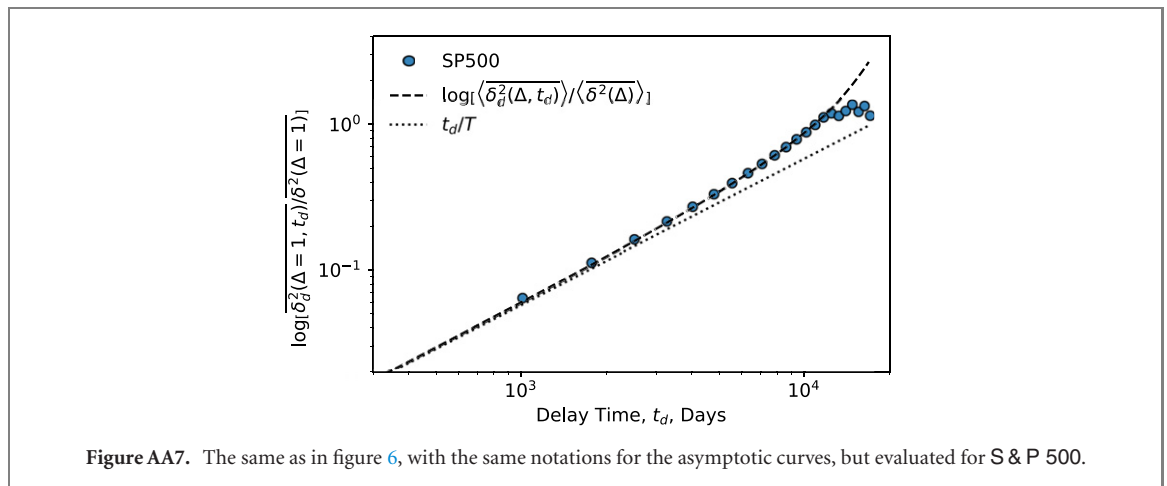
Appendix C. Data-driven assessment of model parameters

Here, we describe the fitting procedures to extract the values of the GBM-model parameters from the historical FTS, see figures AA8 and AA9. In particular, we employ certain fitting and optimization algorithms to determine the stock-specific values of drift μ and volatility σ , used later, e.g., to fit the variations of the delayed TAMSΔ as a function of the delay time t_d .

C1. Optimal ‘valley’ in the $\{\mu, \sigma\}$ -plane

C1.1. Evaluation algorithm

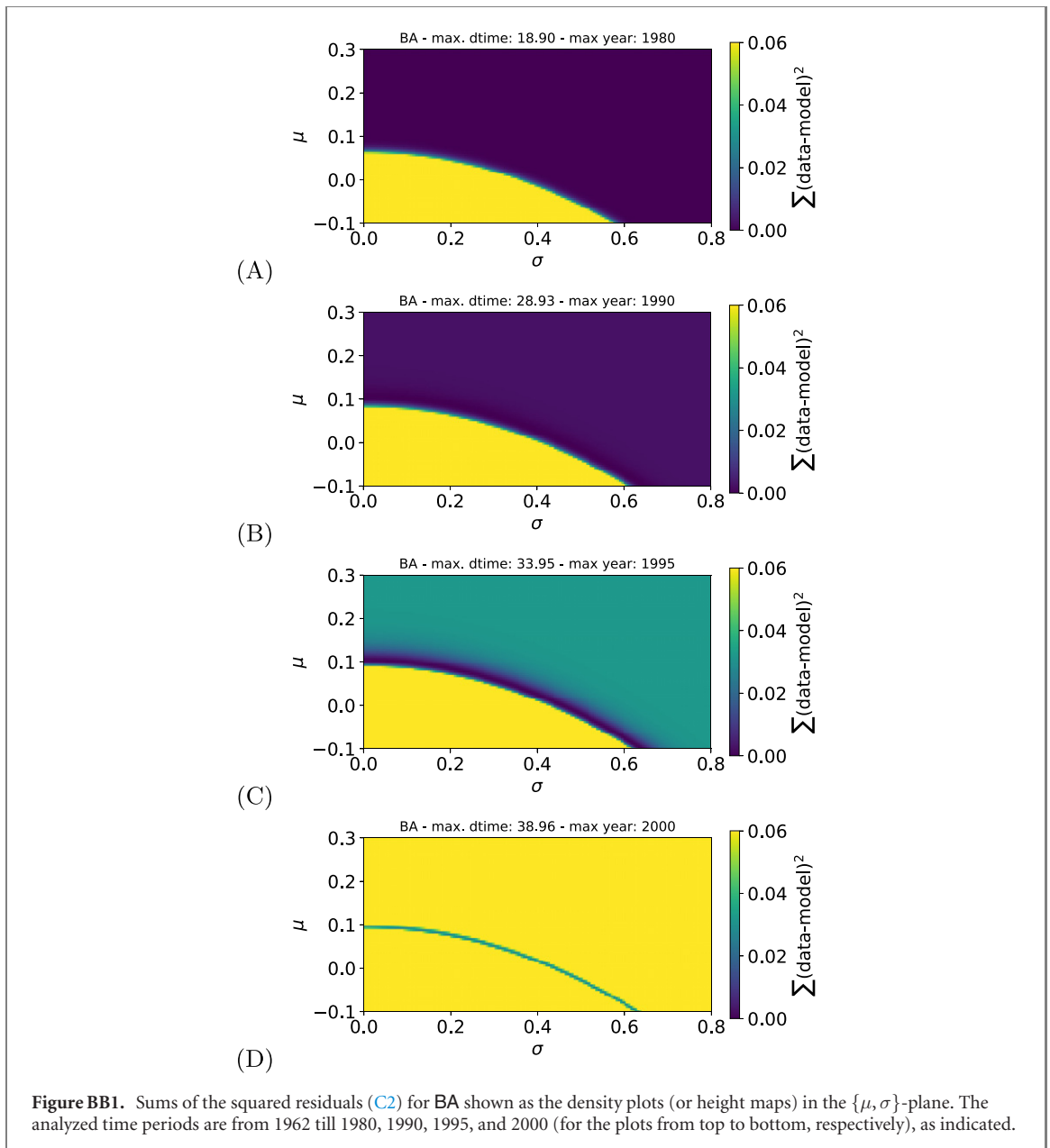
Our fundamental measure, the log-ratio of the delayed versus standard TAMSΔ for all the FTS studied here reveals (in the limit $t_d \ll T$ and short lag times $\Delta \ll T$) a universal parameter-free simple [150] variation given by equation (7). The entire variation of the delayed TAMSΔ given by (27), however, nontrivially depends on the stock-specific drift μ and volatility σ which should be found to fit the whole curve $\delta_{d,i}^2(\Delta)$ versus t_d . A



straightforward *two-parameter fit* of the variation of

$$y_d(\Delta_1) = \log \left[\overline{\delta_d^2}(\Delta_1) / \overline{\delta^2}(\Delta_1) \right] \tag{C1}$$

versus t_d for a given index or stock to find the values of drift and volatility values often yields unsatisfactory results as to the accuracy and consistency of the fit (results not shown). Such a fit is particularly problematic for the FTS encompassing a period of a financial crisis or severe price drops.



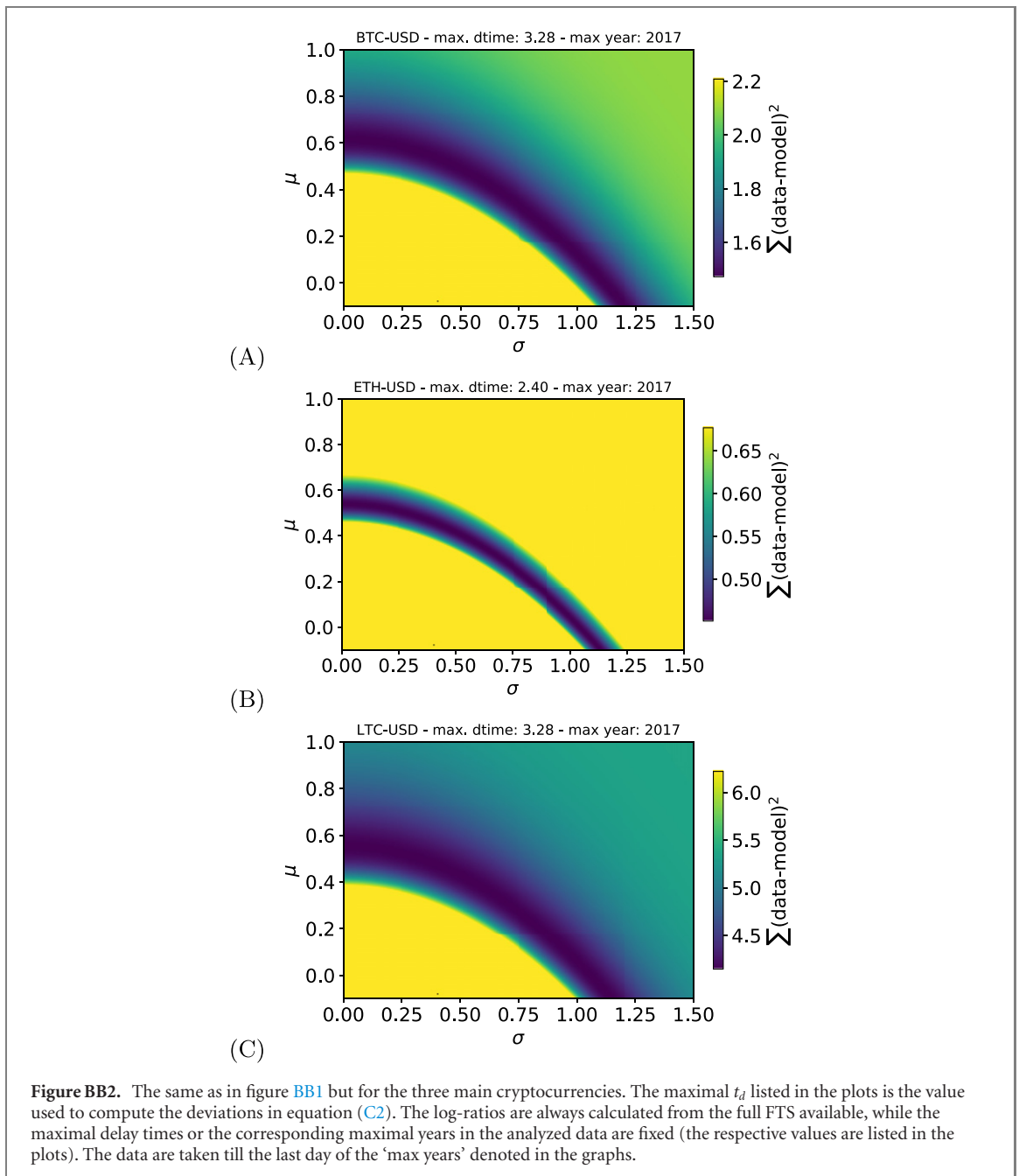
A more rational way to examine the discrepancies between the theoretical GBM-based predictions and real-data results is to compute the sum

$$\sum_{t_d} [y_{d,\text{data}}(\Delta_1) - y_{d,\text{model}}(\Delta_1)]^2 \quad (\text{C2})$$

over all possible values of the delay time t_d (all contributing with equal weights), for systematically varying μ and σ values. The delay time in equation (C2) is sampled with the time-step of $\delta t_d = 1$ day, with the minimal t_d equal to one day (the ‘resolution’ of the FTS used in this study) and the maximal t_d being equal to the preset cutoff time for a given FTS. We compute the squared differences between the log-ratios (C1) for the FTS versus the analytical GBM-based solution for all possible pairs of μ and σ in the preset range (with the discretization step of 0.005) and sum the deviations over all realizable values of t_d . The delayed TAMSDs in (C1) are computed at $\Delta_1 = 1$ day, where statistical averaging over time is most reliable.

C1.2. ‘Classical stocks’

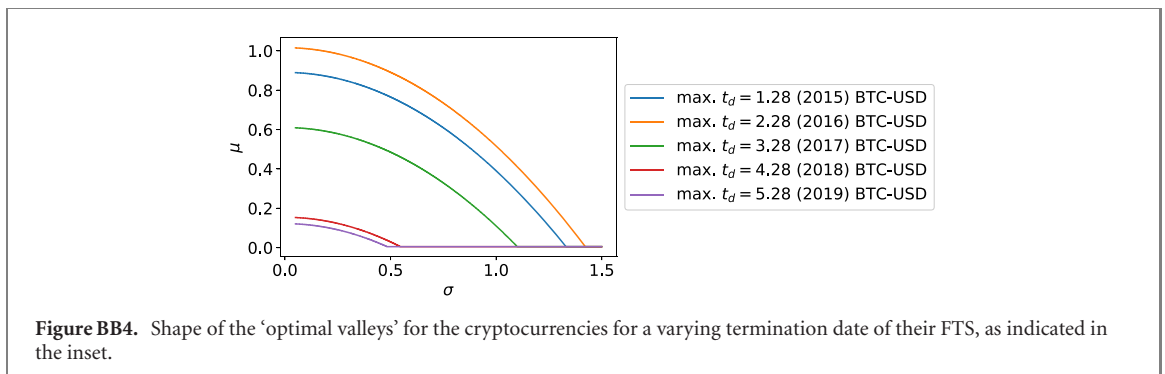
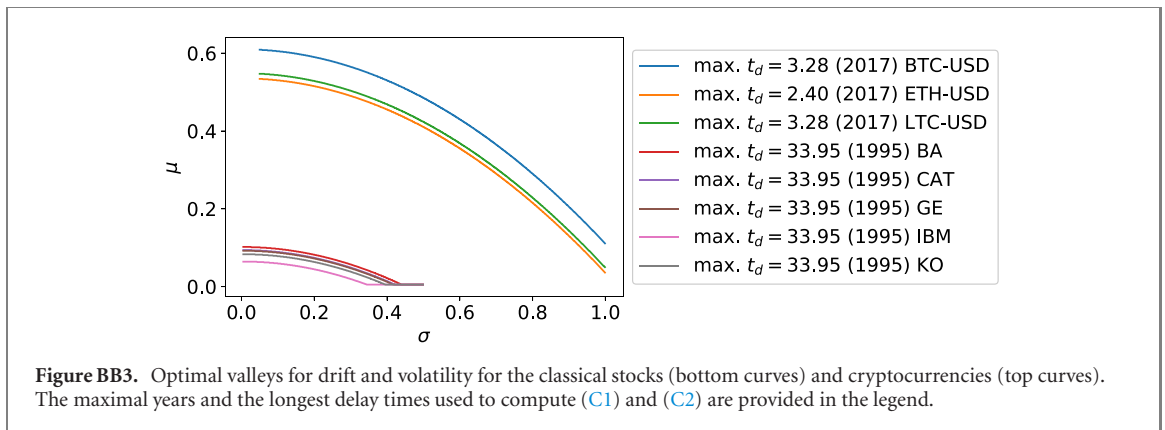
The procedure (C2) gives one point in the $\{\mu, \sigma\}$ plane, see the example of such contour plot for the stock-prices of BA in figure BB1. We find that for all the indices studied the model-versus-data discrepancy quantified by (C2) increases for small σ and small μ values (not shown). In the opposite domain, for large μ and large σ values, the discrepancy increases as well, although often less steeply. At intermediate values of μ and σ an ‘optimal valley’ featuring minimal model-versus-data deviations is often realized, as illustrated in figure BB1.



We find that for the 'classical stocks' the position of this optimal valley in the $\{\mu, \sigma\}$ -plane often does not change strongly upon varying the terminal point of a given FTS and the delay time t_d (a company-universal 'signature'). These plots are the 'fingerprints' reflecting certain functioning principles employed by a given company (in terms of the deterministic μ -based and stochastic σ -based features of resulting variations of its stocks price). The depth of the minimum in figure BB1 for a given valley is an index-specific feature; the depth along the valley often is only *weakly sensitive* to the variations of μ and σ along the 'valley' (results not shown).

C1.3. Cryptocurrencies

In figure BB2 the optimal $\{\mu, \sigma\}$ -valleys for the three main cryptocurrencies are shown. Their $S(t)$ -dynamics is much more rapid and volatile as compared to the classical stocks: the valleys are significantly shifted toward larger values of drift and volatility. In this plot, the data up to the end of 2017 are only considered in the analysis because after this data a number of crashes on the cryptocurrency markets happened and, as a consequence, the results cannot be expected to follow the GBM model. The latter data were, thus, excluded from the analysis of optimal μ and σ values for the cryptocurrencies. This speculation-driven shift of the valley for the cryptocurrencies toward larger μ and σ is also clearly visible in figure BB3. Note that, as cryptocurrencies are traded 24/7, the delay times given in figures BB2–BB4 were recalculated (via multiplying by $\approx 252/365$) to



make them comparable to those for classical stocks (traded for ≈ 252 days per year). One fiscal year and one t_d -year contain, therefore, different numbers of calendar days for classical stocks and cryptocurrencies.

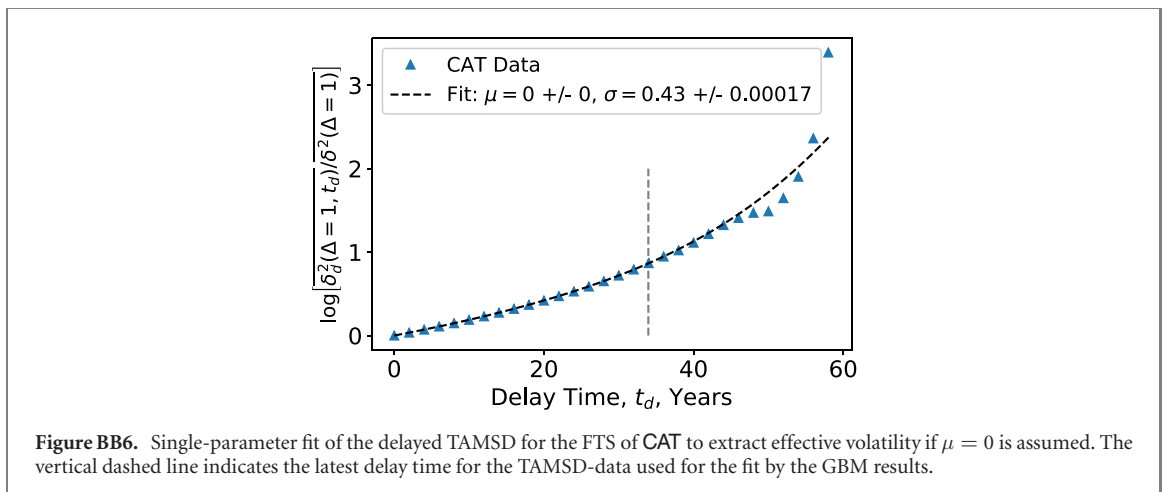
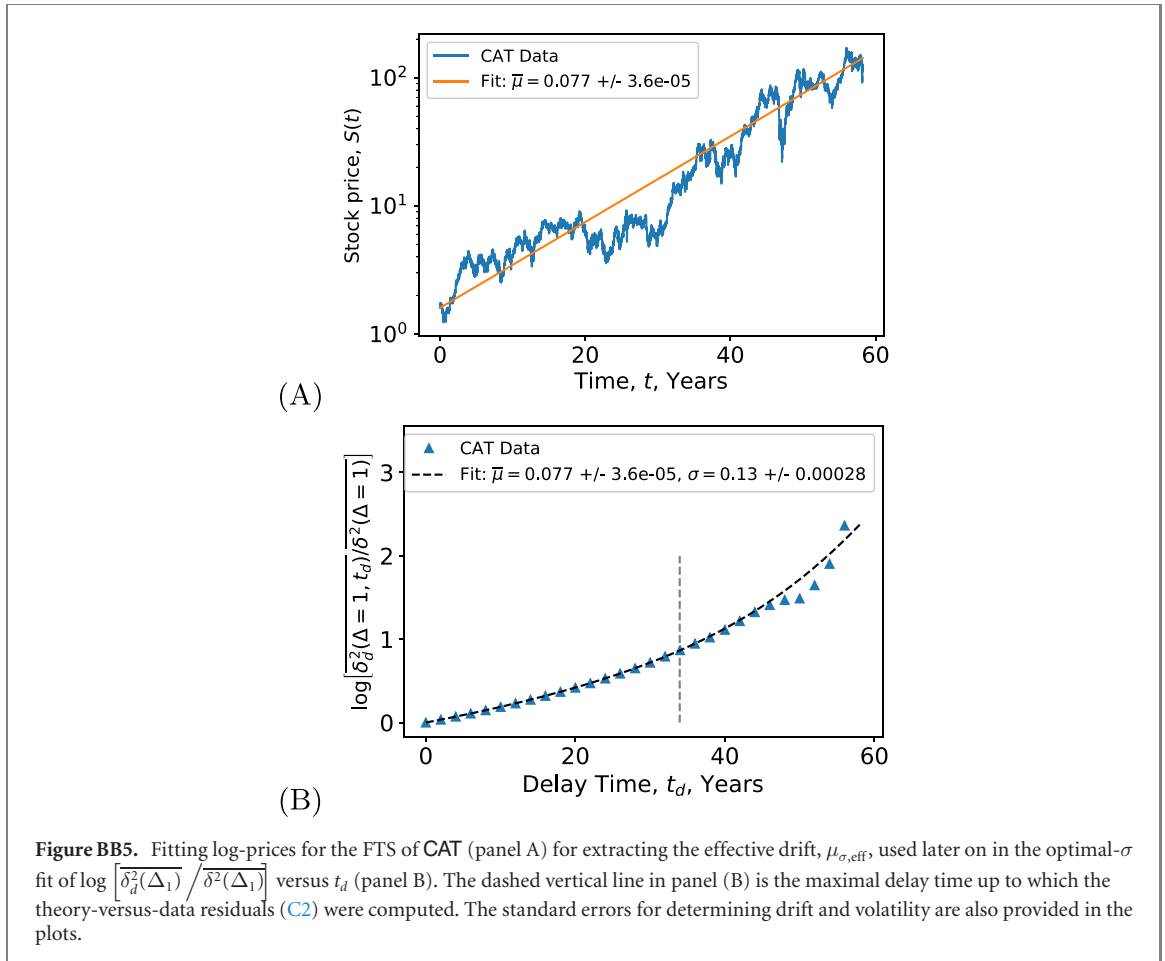
We find that, contrary to the classical and well-established stocks, as shown in figure BB1, for a highly speculative dynamics behind the price evolution of the cryptocurrencies the terminal date of their FTS entering the analysis of equation (C2) indeed *changes* the location of the optimal $\{\mu, \sigma\}$ -valley. Specifically, when the latest data for BitCoin or BTC are included in the analysis, the position of the optimal valley shifts toward lower drift and volatility values, see figure BB4. This likely is a manifestation of a 'cooling down' effect after the crash in late December 2017 (as well as several later drops of the BitCoin price in the period 2018–2020) that made cryptocurrencies generally less promising for speculative short-term 'in-and-out' investments during those periods. In contrast, the optimal valleys for the 'heating-up' phase in the dynamics of the cryptocurrencies (with the terminal years being 2015 and 2016 in figure BB4) are located in the range of considerably *larger* values of drift and volatility (artificial price 'heating-up' as a preparation for a later crash of the pyramid and to extraction of profits).

These features of the $\{\mu, \sigma\}$ -plots in figures BB2 and BB3 may be viewed as some speculative instruments enabling 'big players' to control, manipulate, and direct the market, while 'small players' can only react to trends/news. Such small investors act delayed, the disadvantage vital for highly volatile markets of cryptocurrencies. Additional (natural or artificial) delays in the BitCoin selling scheme—like those occurred during the super-hype with sky-rocketing BitCoin prices in late December 2017, with lag times of up to a *week*(!) [198] required to complete the transactions—further impede small investors from timely monetizing their profits.

The minimum in the optimal $\{\mu, \sigma\}$ -valley is often attained for an infinite set of μ -and- σ pairs, with a certain functional connectivity. This 'over-determination' or 'degeneracy' of parameters, not surprising for a two-parameter fit, suggests a better strategy, where one parameter is determined directly from the data (μ), while another one (σ) is then found from the computed 'optimal valleys', see appendix C2.

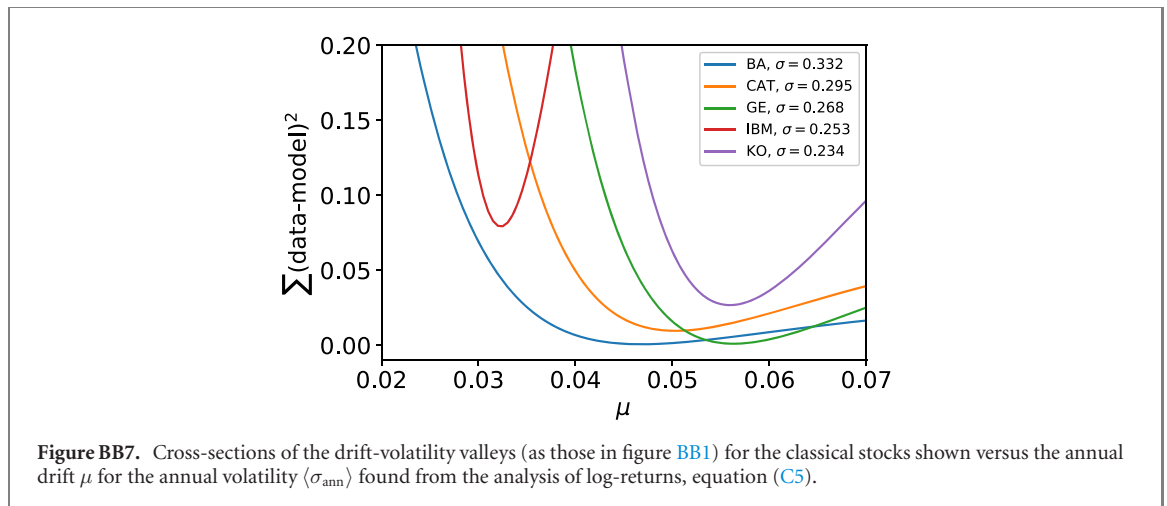
C2. Fitting $\overline{\delta_{d,i}^2(\Delta)}$ data and optimal $\{\mu, \sigma\}$ -valley

The value of μ can be found via direct linear fit of $\log[S_i(t)]$ versus t for a given stock in the same time domain as used previously to calculate $\overline{\delta_{d,i}^2(\Delta)}$. In virtue of a roughly exponential price evolution of $S(t)$ (if described by GBM and after neglecting the σ -containing term in (11)), one can estimate the effective drift $\mu_{\sigma, \text{eff}}$ (36) and using the landscape of the 'optimal valley' find the company-specific value of volatility. In figure BB5 the linear fit of $\log[S(t)]$ for CAT is presented. Note here a considerable arbitrariness in the length of the FTS used



for the fit and certain uncertainties with regard, e.g., to the value of $\log[S(t)]$ rapidly changing in magnitude. This procedure gives reasonable estimates and errors for the optimal μ and σ for some of the FTS examined.

However, for the value of μ estimated this way no uniquely corresponding value of σ can sometimes be found from the $\{\mu, \sigma\}$ -contour plots. Moreover, the contour plots of GBM-versus-data residuals (C2) for all the indices studied (results not shown) indicate that estimating σ from the data first and finding the respective value of μ afterward can be a more appropriate procedure, see appendix C3. Note that some more ‘local’ estimates for μ of GBM can be obtained via fitting $\log[S(t)]$ not for the whole FTS-data available, but rather, e.g., only for a crash-free time-domain (provided the GBM model is applicable there). Lastly, one can in principle set $\mu = 0$ and (for most indices) find the corresponding volatility via a one-parameter fit, see figure BB6 for CAT.



C3. Assessment of parameters using log-returns

A more strict and also previously used [199] procedure is to determine σ first using the concept of time-local log-returns. The latter, defined at discrete times t_n along a given FTS $S(t)$ as

$$r(t_n) = \log[S(t_n)/S(t_{n-1})], \tag{C3}$$

presents a standard quantifier of price fluctuations of a stocks index. The log in (C3) ‘removes’ the expected exponential growth of price in time (supposing $S(t)$ develops according to GBM). For small price variations the log-returns (C3) approach the standard returns, r_n . The cross-sectional standard deviation of returns defines the dispersion of individual returns with respect to the mean for a given period of time, the averaging window. During periods of market stress [145], the dispersion should increase due to higher volatilities of rapidly fluctuating prices, but the herding behavior has, in contrast, an opposite impact: people tend to follow the trends thus reducing the dispersion [145, 200].

The average volatility $\langle\sigma\rangle$ for all \bar{N} points used in the analysis of a given FTS is given through the trajectory-average return defined as

$$\langle r \rangle = \frac{1}{\bar{N} - 1} \sum_{n=2}^{\bar{N}} r(t_n) \tag{C4}$$

by [199]

$$\langle \sigma \rangle = \sqrt{\frac{1}{\bar{N} - 1} \sum_{n=2}^{\bar{N}} [r(t_n) - \langle r \rangle]^2}. \tag{C5}$$

We calculate $\langle\sigma\rangle$ from the daily FTS with $\Delta t = 1/252$ (for ≈ 252 trading days per year [for the classical stocks]). The annual volatility is then

$$\langle\sigma_{\text{ann}}\rangle = \langle\sigma\rangle / \sqrt{\Delta t} = \sqrt{252} \langle\sigma\rangle. \tag{C6}$$

Clearly, via using (C5) one can also compute the volatility for each year of the FTS-data separately if, e.g., time-dependent annual features of the price-evolution dynamics are to be considered.

Plotting the variation of the squared residuals (C2) versus μ for the volatility value found from (C5) for each of the FTS we easily find a unique value of the drift parameter μ , as illustrated in figure BB7 (due to the existence of a clear minimum for the curve). This method provides a direct, rational, and unique way to find the optimal pair of drift-and-volatility for a given FTS and in an arbitrary time-domain making the current method superior to the approaches discussed in appendices C1 and C2).

The parabolic-looking curves in figure BB7 represent the cross-sections of the two-dimensional plots of figure BB1 for the same index/company after one has set the volatility to $\sigma = \langle\sigma\rangle$ given by equation (C5) for each of the stocks. The parameters μ and σ are bound to the time unit used in data-based computation and simulations¹¹. We observe, e.g., that a sharper minimum for IBM in figure BB7 symbolizes a smaller ‘tolerance’

¹¹ If time is in years (as in most of our simulations in section 4, or $t = 1/252$ being one day), then μ is the yearly (‘per annum’) interest rate and σ is the annual volatility (for classical stocks). Thus, if not stated otherwise, we always refer to the *annual* values of μ and σ to compare the outcomes to the results of GBM simulations. The volatility—defined as the standard deviation of log returns, distributed normally with $\mathcal{N}((\mu - \sigma^2/2)t; \sigma^2 t)$ for GBM, equation (34)—scales with $\sqrt{\text{time window}}$. To compute ‘annual’ volatility, we can calculate the standard deviation from the yearly log-returns for sample size $N = 60$ (for a 60 years-long FTS), or from the daily log-returns for the same data with the sample size $N = 15120$ days and then scale the value with $\sqrt{252}$ (for ‘classical’ stocks), as in equation (C6).

of this index (in a given time domain) to deviations of parameters. Namely, upon variation of the drift parameter the GBM-based predictions for the delayed TAMSD quickly deviate from the determined minimum. This sharp minimum corroborates the behavior of the squared residuals (C2) for IBM when visualized as the density plots in the $\{\mu, \sigma\}$ -plane (not shown).

ORCID iDs

Andrey G Cherstvy  <https://orcid.org/0000-0002-0516-9900>

Ralf Metzler  <https://orcid.org/0000-0002-6013-7020>

References

- [1] Bachelier L 1900 Théorie de la spéculation *Ann. Sci. Ecole Norm. Supérieure* **17** 21
Bachelier L 1964 *The Random Character of Stock Market Prices* ed P Cootner (Cambridge, MA: MIT Press) pp 17–78 (Engl. transl.)
- [2] Bronzin V 1908 *Theorie der Prämiengeschäfte* (Leipzig und Wien: Verlag Franz Deticke)
- [3] Fama E F 1965 The behavior of stock-market prices *J. Bus.* **38** 34
- [4] Samuelson P A 1965 Proof that properly anticipated prices fluctuate randomly *Ind. Manag. Rev.* **6** 41
- [5] Fama E F 1998 Market efficiency, long-term returns, and behavioral finance *J. Financ. Econ.* **49** 283
- [6] Bachelier L 1912 *Calcul des Probabilités* (Paris: Gauthier-Villars)
- [7] Hafner W and Zimmermann H 2009 *Vinzenz Bronzin's Option Pricing Models: Exposition and Appraisal* (Berlin: Springer)
- [8] Sprengle C 1961 Warrant prices as indications of expectations *Yale Econ. Essays* **1** 178
- [9] Mandelbrot B 1963 The variation of certain speculative prices *J. Bus.* **36** 394
- [10] Mandelbrot B 1963 New methods in statistical economics *J. Polit. Econ.* **71** 421
- [11] Boness A J 1964 Elements of a theory of stock-option value *J. Polit. Econ.* **72** 163
- [12] Samuelson P A 1965 Rational theory of warrant pricing *Ind. Manag. Rev.* **6** 13
- [13] Kendall M G and Hill A B 1953 The analysis of economic time-series-part: I. Prices *J. R. Stat. Soc. A* **116** 11
- [14] Osborne M F M 1959 Brownian motion in the stock market *Oper. Res.* **7** 145
- [15] Mandelbrot B 1966 Forecasts of future prices, unbiased markets, and martingale models *J. Bus.* **39** 242
- [16] Fama E F, Fisher L, Jensen M C and Roll R 1969 The adjustment of stock prices to new information *Int. Econ. Rev.* **10** 1
- [17] Thorp E O 1969 Optimal gambling systems for favorable games *Rev. Inst. Int. Stat.* **37** 273
- [18] Samuelson P A and Merton R C 1969 A complete model of warrant pricing that maximizes utility *Ind. Manag. Rev.* **10** 17
- [19] Fama E F 1970 Efficient capital markets: a review of theory and empirical work *J. Finance* **25** 383
- [20] Merton R C 1971 Optimum consumption and portfolio rules in a continuous-time model *J. Econ. Theor.* **3** 373
- [21] Black F and Scholes M 1972 The valuation of option contracts and a test of market efficiency *J. Finance* **27** 399
- [22] Black F and Scholes M 1973 The pricing of options and corporate liabilities *J. Polit. Econ.* **81** 637
- [23] Merton R C 1973 Theory of rational option pricing *Bell J. Econ. Manag. Sci.* **4** 141
- [24] Merton R C 1974 On the pricing of corporate debt: the risk structure of interest rates *J. Finance* **29** 449
- [25] Merton R C 1976 Option pricing when underlying stock returns are discontinuous *J. Financ. Econ.* **3** 125
- [26] Black F 1989 How we came up with the option formula *J. Portfolio Manag.* **15** 4
- [27] Fama E F 1991 Efficient capital markets: II *J. Finance* **46** 1575
- [28] Cox J C and Ross S A 1976 The valuation of options for alternative stochastic processes *J. Financ. Econ.* **3** 145
- [29] Vasicek O 1977 An equilibrium characterization of the term structure *J. Financ. Econ.* **5** 177
- [30] Cox J C, Ross S A and Rubinstein M 1979 Option pricing: a simplified approach *J. Financ. Econ.* **7** 229
- [31] Geske R 1979 The valuation of compound options *J. Financ. Econ.* **7** 63
- [32] Cox J C, Ingersoll J E Jr and Ross S A 1985 A theory of the term structure of interest rates *Econometrica* **53** 385
- [33] Hull J and White A 1987 The pricing of options on assets with stochastic volatilities *J. Finance* **42** 281
- [34] Johnson H and Shanno D 1987 Option pricing when the variance is changing *J. Financ. Quant. Anal.* **22** 143
- [35] Ross S A 1989 Information and volatility: the no-arbitrage martingale approach to timing and resolution irrelevancy *J. Finance* **44** 1
- [36] Heston S L 1993 A closed-form solution for options with stochastic volatility with applications to bond and currency options *Rev. Financ. Stud.* **6** 327
- [37] Rubinstein M 1994 Implied binomial trees *J. Finance* **49** 771
- [38] Cox J C 1996 The constant elasticity of variance option pricing model *J. Portfolio Manag.* **23** 15
- [39] Boyle P P and Tian Y 1999 Pricing lookback and barrier options under the CEV process *J. Financ. Quant. Anal.* **34** 241
- [40] Merton R C 1998 Applications of option-pricing theory: twenty-five years later *Am. Econ. Rev.* **88** 323
- [41] Duffie D, Pan J and Singleton K 2000 Transform analysis and asset pricing for affine jump-diffusions *Econometrica* **68** 1343
- [42] Campbell J Y 2000 Asset pricing at the millennium *J. Finance* **55** 1569
- [43] Sundaresan S M 2000 Continuous-time methods in finance: a review and an assessment *J. Finance* **55** 1515
- [44] Heston S L and Nandi S 2000 A closed-form GARCH option valuation model *Rev. Financ. Stud.* **13** 585
- [45] Acharya V and Pedersen L 2005 Asset pricing with liquidity risk *J. Financ. Econ.* **77** 375
- [46] Samuelson P 1947 *Foundations of Economic Analysis* (Cambridge, MA: Harvard University Press)
- [47] Thorp E O and Kassouf S T 1967 *Beat the Market* (New York: Random House)
- [48] Cootner P H 1967 *The Random Character of Stock Market Prices* (Cambridge, MA: MIT Press)
- [49] Auster R 1975 *Option Writing and Hedging Strategies* (New York: Exposition Press)
- [50] Ingersoll J E Jr 1986 *Theory of Financial Decision Making* (New Haven, CT: Yale University Press)
- [51] Hull J C 1996 *Options, Futures, and Other Derivative Securities* 3rd edn (Englewood Cliffs, NJ: Prentice-Hall)
- [52] Mandelbrot B B 1997 *Fractals and Scaling in Finance Selecta Volume E* (Berlin: Springer)
- [53] Campbell J Y, Lo A W and MacKinlay A C 1997 *The Econometrics of Financial Markets* (Princeton, NJ: Princeton University Press)

- [54] Hull J C 1997 *Options, Futures and Other Derivates* 3rd edn (Englewood Cliffs, NJ: Prentice-Hall)
- [55] Mantegna R N and Stanley H E 2000 *An Introduction to Econophysics: Correlations and Complexity in Finance* (Cambridge: Cambridge University Press)
- [56] Bouchaud J-P and Potters M 2000 *Theory of Financial Risk and Derivative Pricing: From Statistical Physics to Risk Management* (Cambridge: Cambridge University Press)
- [57] Fouque J-P, Papanicolaou G and Sircar K R 2000 *Derivative in Financial Markets with Stochastic Volatility* (Cambridge: Cambridge University Press)
- [58] Duffie D 2001 *Dynamic Asset Pricing Theory* 3rd edn (Princeton, NJ: Princeton University Press)
- [59] Takayasu H (ed) 2004 *The application of econophysics Proc. Second Nikkei Econophysics Symposium* (Berlin: Springer)
- [60] Gatheral J 2006 *Stochastic Volatility Modeling* (New York: Wiley)
- [61] McCauley J L 2009 *Dynamics of Markets: The New Financial Economics* (Cambridge: Cambridge University Press)
- [62] McCauley J L 2013 *Stochastic Calculus and Differential Equations for Physics and Finance* (Cambridge: Cambridge University Press)
- [63] Derman E and Miller M B 2016 *The Volatility Smile* (New York: Wiley)
- [64] Johnson H and Shanno D 1987 Option pricing when the variance is changing *J. Financ. Quant. Anal.* **22** 143
- [65] Haug E G and Taleb N N 2011 Option traders use (very) sophisticated heuristics, never the Black–Scholes–Merton formula *J. Econ. Behav. Organ.* **77** 97
- [66] Kou S G 2002 A jump-diffusion model for option pricing *Manag. Sci.* **48** 955
- [67] Kou S G and Wang H 2003 First passage times of a jump diffusion process *Adv. Appl. Probab.* **35** 504
- [68] Kou S G and Wang H 2004 Option pricing under a double exponential jump diffusion model *Manag. Sci.* **50** 1178
- [69] Feng L and Linetsky V 2008 Pricing options in jump-diffusion models: an extrapolation approach *Oper. Res.* **56** 304
- [70] Fusai G and Meucci A 2008 Pricing discretely monitored Asian options under Lévy processes *J. Bank. Finance* **32** 2076
- [71] Hawkes A G 2020 Hawkes jump-diffusions and finance: a brief history and review *Eur. J. Finance* <https://doi.org/10.1080/1351847x.2020.1755712>
- [72] Madan D B, Carr P P and Chang E C 1998 The variance gamma process and option pricing *Eur. Finance Rev.* **2** 79
- [73] Carr P, Geman H, Madan D B and Yor M 2003 Stochastic volatility for Levy processes *Math. Finance* **13** 345
- [74] Broadie M, Glasserman P and Kou S G 1999 Connecting discrete and continuous path-dependent options *Finance Stochast.* **3** 55
- [75] Fallahgoul H A, Focardi S M and Fabozzi F J 2017 *Fractional Calculus and Fractional Processes with Applications to Financial Economics: Theory and Application* (Amsterdam: Elsevier)
- [76] Cutler D M, Poterba J M and Summers L H 1991 Speculative dynamics *Rev. Econ. Stud.* **58** 529
- [77] Hsu S 2017 *Financial Crises, 1929 to the Present* 2nd edn (Edward Elgar Publishing)
- [78] Sornette D 2014 Physics and financial economics (1776–2014): puzzles, Ising and agent-based models *Rep. Prog. Phys.* **77** 062001
- [79] Sornette D 2003 Critical market crashes *Phys. Rep.* **378** 1
- [80] Sornette D, Woodard R and Zhou W-X 2009 The 2006–2008 oil bubble: evidence of speculation, and prediction *Physica A* **388** 1571
- [81] Zhou W-X and Sornette D 2006 Is there a real-estate bubble in the US? *Physica A* **361** 297
- [82] Kristoufek L 2013 BitCoin meets Google Trends and Wikipedia: quantifying the relationship between phenomena of the Internet era *Sci. Rep.* **3** 3415
- [83] Bouri E, Gupta R and Roubaud D 2019 Herding behaviour in cryptocurrencies *Finance Res. Lett.* **29** 216
- [84] Gerlach J C, Demos G and Sornette D 2019 Dissection of Bitcoin’s multiscale bubble history from January 2012 to February 2018 *R. Soc. Open Sci.* **6** 180643
- [85] Taleb N N 2007 *The Black Swan: The Impact of the Highly Improbable* (New York: Random House)
- [86] Bouchaud J-P, Farmer J D and Lillo F 2009 How markets slowly digest changes in supply and demand *Handbook of Financial Markets: Dynamics and Evolution* (Amsterdam: North-Holland) ch 2
- [87] Black F and Cox J C 1976 Valuing corporate securities: some effects of bond indenture provisions *J. Finance* **31** 351
- [88] Bouchaud J-P 2008 Economics needs a scientific revolution *Nature* **455** 1181
- [89] Dragulescu A A and Yakovenko V M 2002 Probability distribution of returns in the Heston model with stochastic volatility *Quant. Finance* **2** 443
- [90] Pirjol D, Jafarpour F and Iyer-Biswas S 2017 Phenomenology of stochastic exponential growth *Phys. Rev. E* **95** 062406
- [91] Iyer-Biswas S et al 2014 Scaling laws governing stochastic growth and division of single bacterial cells *Proc. Natl Acad. Sci. USA* **111** 15912
- [92] Bouchaud J-P and Sornette D 1994 The Black–Scholes option pricing problem in mathematical finance: generalization and extensions for a large class of stochastic processes *J. Phys. I France* **4** 863
- [93] Bouchaud J-P 2005 The subtle nature of financial random walks *Chaos* **15** 026104
- [94] Magdziarz M 2009 Black–Scholes formula in subdiffusive regime *J. Stat. Phys.* **136** 553
- [95] Orzel S and Weron A 2010 Calibration of the subdiffusive Black–Scholes model *Acta Phys. Pol. B* **41** 1151
- [96] Angstmann C N, Henry B I and McGann A V 2019 Time-fractional geometric Brownian motion from continuous time random walks *Physica A* **526** 121002
- [97] Dhesi G, Shakeel B and Ausloos M 2021 Modelling and forecasting the kurtosis and returns distributions of financial markets: irrational fractional Brownian motion model approach *Ann. Oper. Res.* **299** 1397
- [98] Mishura Y S, Piterbarg V I, Ralchenko K V and Yurchenko-Tytarenko A Y 2018 Stochastic representation and path properties of a fractional Cox–Ingersoll–Ross process *Theor. Probab. Math. Stat.* **97** 167
- [99] Hu Y and Øksendal B 2003 Fractional white noise calculus and applications to finance *Infinite Dimens. Anal., Quantum Probab. Relat. Top.* **6** 1
- [100] Stojkoski V, Sandev T, Basnarkov L, Kocarev L and Metzler R 2020 Generalised geometric Brownian motion: theory and applications to option pricing *Entropy* **22** 1432
- [101] Krzyzanowski G and Magdziarz M 2021 A computational weighted finite difference method for American and barrier options in subdiffusive Black–Scholes model *Commun. Nonlinear Sci. Numer. Simul.* **96** 105676
- [102] Stanislavsky A A 2003 Black–Scholes model under subordination *Physica A* **318** 474
- [103] Magdziarz M and Gajda J 2012 Anomalous dynamics of Black–Scholes model time-changed by inverse subordinators *Acta Phys. Pol. B* **43** 1093
- [104] Scalas E 2006 The application of continuous-time random walks in finance and economics *Physica A* **362** 225
- [105] Meerschaert M M and Scalas E 2006 Coupled continuous time random walks in finance *Physica A* **370** 114

- [106] Magdziarz M, Orzel S and Weron A 2011 Option pricing in subdiffusive Bachelier model *J. Stat. Phys.* **145** 187
- [107] Scalas E 2006 Five years of continuous-time random walks in econophysics *The Complex Networks of Economic Interactions Lecture Notes in Economics and Mathematical Systems* vol 567, ed A Namatame, T Kaizouji and Y Aruka (Berlin: Springer)
- [108] Li C 2016 Option pricing with generalized continuous time random walk models PhD Thesis University of London
- [109] Lebowitz J L and Penrose O 1973 Modern ergodic theory *Phys. Today* **26** 23
- [110] Bouchaud J P 1992 Weak ergodicity breaking and aging in disordered systems *J. Phys. I France* **2** 1705
- [111] Moore C C 2015 Ergodic theorem, ergodic theory, and statistical mechanics *Proc. Natl Acad. Sci. USA* **112** 1907
- [112] Peters O 2011 Optimal leverage from non-ergodicity *Quant. Finance* **11** 1593
- [113] Peters O and Klein W 2013 Ergodicity breaking in geometric Brownian motion *Phys. Rev. Lett.* **110** 100603
- [114] Peters O 2019 The ergodicity problem in economics *Nat. Phys.* **15** 1216
- [115] Bouchaud J-P and Farmer R E A 2020 Self-fulfilling prophecies, quasi non-ergodicity, and wealth inequality (arXiv:2012.09445)
- [116] Doctor J N, Wakker P P and Wang T V 2020 Economists' views on the ergodicity problem *Nat. Phys.* **16** 1168
- [117] Gadenne F 2020 Ergodicity economics in plain english *Retire. Manag. J.* **9** 61
- [118] Grossman S J and Stiglitz J E 1980 On the impossibility of informationally efficient markets *Am. Econ. Rev.* **70** 393
- [119] Engle R F and Ng V K 1993 Measuring and testing the impact of news on volatility *J. Finance* **48** 1749
- [120] Black F 1986 Noise *J. Finance* **41** 530
- [121] Kahneman D and Tversky A 1979 Prospect theory: an analysis of decision under risk *Econometrica* **47** 263
- [122] Shiller R J 1999 Human behavior and the efficiency of the financial system *Handbook of Macroeconomics* vol 1 ed J B Taylor and M Woodford (Amsterdam: Elsevier Science B. V.) pp 1305–40 ch 20
- [123] Shiller R J 2003 From efficient markets theory to behavioral finance *J. Econ. Perspect.* **17** 83
- [124] Shleifer A 2000 *Inefficient Markets: An Introduction to Behavioural Finance Clarendon Lectures in Economics* (Oxford: Oxford University Press)
- [125] Bouchaud J-P, Gefen Y, Potters M and Wyart M 2004 Fluctuations and response in financial markets: the subtle nature of 'random' price changes *Quant. Finance* **4** 176
- [126] Aydiner E, Cherstvy A G and Metzler R 2018 Wealth distribution, Pareto law, and stretched exponential decay of money: computer simulations analysis of agent-based models *Physica A* **490** 278
- [127] French K R and Roll R 1986 Stock return variances: the arrival of information and the reaction of traders *J. Financ. Econ.* **17** 5
- [128] Stiglitz J E 2002 Information and the change in the paradigm in economics *Am. Econ. Rev.* **92** 460
- [129] Rothschild M and Stiglitz J 1976 Equilibrium in competitive insurance markets: an essay on the economics of imperfect information *Q. J. Econ.* **90** 629
- [130] Grossman S J and Stiglitz J E 1976 Information and competitive price systems *Am. Econ. Rev.* **66** 246
- [131] Shiller R J 1981 Do stock prices move too much to be justified by subsequent changes in dividends? *Am. Econ. Rev.* **71** 421
- [132] Cutler D M, Poterba J M and Summers L H 1989 What moves stock prices? *J. Portfolio Manag.* **15** 4
- [133] Summers L H 1986 Does the stock market rationally reflect fundamental values? *J. Finance* **41** 591
- [134] Shefrin H and Statman M 1994 Behavioral capital asset pricing theory *J. Financ. Quant. Anal.* **29** 323
- [135] de Bondt W F M and Thaler R 1985 Does the stock market overreact? *J. Finance* **40** 793
- [136] Lo A W and MacKinlay A C 1988 Stock market prices do not follow random walks: evidence from a simple specification test *Rev. Financ. Stud.* **1** 41
- [137] Lo A W and MacKinlay A C 1999 *A Non-random Walk Down Wall Street* (Princeton, NJ: Princeton University Press)
- [138] Malkiel B G 2003 The efficient market hypothesis and its critics *J. Econ. Perspect.* **17** 59
- [139] Sornette D 2003 *Why Stock Markets Crash: Critical Events in Complex Financial Systems* (Princeton, NJ: Princeton University Press)
- [140] Giardina I and Bouchaud J-P 2003 Bubbles, crashes and intermittency in agent based market models *Eur. Phys. J. B* **31** 421
- [141] Johansen A and Sornette D 2000 The Nasdaq crash of April 2000: yet another example of log-periodicity in a speculative bubble ending in a crash *Eur. Phys. J. B* **17** 319
- [142] Jiang Z-Q, Zhou W-X, Sornette D, Woodard R, Bastiaensen K and Cauwels P 2010 Bubble diagnosis and prediction of the 2005–2007 and 2008–2009 Chinese stock market bubbles *J. Econ. Behav. Organ.* **74** 149
- [143] Lux T 1995 Herd behaviour, bubbles and crashes *Econ. J.* **105** 881
- [144] Cont R and Bouchaud J-P 2000 Herd behavior and aggregate fluctuations in financial markets *Macroecon. Dyn.* **4** 170
- [145] Christie W G and Huang R D 1995 Following the pied piper: do individual returns herd around the market? *Financ. Anal. J.* **51** 31
- [146] Bouri E, Gupta R and Roubaud D 2019 Herding behaviour in cryptocurrencies *Finance Res. Lett.* **29** 216
- [147] Hüsler A, Sornette D and Hommes C H 2013 Super-exponential bubbles in lab experiments: evidence for anchoring over-optimistic expectations on price *J. Econ. Behav. Organ.* **92** 304
- [148] Kreuser J and Sornette D 2019 Super-exponential RE bubble model with efficient crashes *Eur. J. Finance* **25** 338
- [149] Poterba J M and Summers L H 1988 Mean reversion in stock prices *J. Financ. Econ.* **22** 27
- [150] Cherstvy A G, Vinod D, Aghion E, Chechkin A V and Metzler R 2017 Time averaging, ageing and delay analysis of financial time series *New J. Phys.* **19** 063045
- [151] Cherstvy A G et al 2021 Ergodic properties of geometric Brownian motion (work in progress)
- [152] Schenzle A and Brand H 1979 Multiplicative stochastic processes in statistical physics *Phys. Rev. A* **20** 1628
- [153] Oksendal B 2010 *Stochastic Differential Equations: An Introduction with Applications* 6th edn (Berlin: Springer)
- [154] Burov S, Jeon J-H, Metzler R and Barkai E 2011 Single particle tracking in systems showing anomalous diffusion: the role of weak ergodicity breaking *Phys. Chem. Chem. Phys.* **13** 1800
- [155] Metzler R, Jeon J-H, Cherstvy A G and Barkai E 2014 Anomalous diffusion models and their properties: non-stationarity, non-ergodicity, and ageing at the centenary of single particle tracking *Phys. Chem. Chem. Phys.* **16** 24128
- [156] Manzo C and Garcia-Parajo M F 2015 A review of progress in single particle tracking: from methods to biophysical insights *Rep. Prog. Phys.* **78** 124601
- [157] Cherstvy A G and Metzler R 2014 Nonergodicity, fluctuations, and criticality in heterogeneous diffusion processes *Phys. Rev. E* **90** 012134
- [158] Bodrova A, Chechkin A V, Cherstvy A G and Metzler R 2015 Quantifying non-ergodic dynamics of force-free granular gases *Phys. Chem. Chem. Phys.* **17** 21791
- [159] Safdari H, Cherstvy A G, Chechkin A V, Thiel F, Sokolov I M and Metzler R 2015 Quantifying the non-ergodicity of scaled Brownian motion *J. Phys. A: Math. Theor.* **48** 375002

- [160] Cherstvy A G and Metzler R 2015 Ergodicity breaking, ageing, and confinement in generalized diffusion processes with position and time dependent diffusivity *J. Stat. Mech.* [P05010](#)
- [161] Cherstvy A G, Wang W, Metzler R and Sokolov I M 2021 Inertia triggers nonergodicity of fractional Brownian motion *Phys. Rev. E* **104** 024115
- [162] Cherstvy A G, Thapa S, Mardoukhi Y, Chechkin A V and Metzler R 2018 Time averages and their statistical variation for the Ornstein–Uhlenbeck process: role of initial particle conditions and relaxation to stationarity *Phys. Rev. E* **98** 022134
- [163] Wang W, Cherstvy A G, Chechkin A V, Thapa S, Seno F, Liu X and Metzler R 2020 Fractional Brownian motion with random diffusivity: emerging residual nonergodicity below the correlation time *J. Phys. A: Math. Theor.* **53** 474001
- [164] Cherstvy A G, Safdari H and Metzler R 2021 Anomalous diffusion, nonergodicity, and ageing for exponentially and logarithmically time-dependent diffusivity: striking differences for massive versus massless particles *J. Phys. D: Appl. Phys.* **54** 195401
- [165] Vinod D, Cherstvy A G, Wang W, Metzler R and Sokolov I M Nonergodicity of reset geometric Brownian motion (in preparation)
- [166] Wang W, Cherstvy A G, Kantz H, Metzler R and Sokolov I M 2021 Time-averaging and emerging nonergodicity upon resetting of fractional Brownian motion and heterogeneous diffusion processes *Phys. Rev. E* **104** 024105
- [167] Cherstvy A G, Vinod D, Aghion E, Sokolov I M and Metzler R 2021 Scaled geometric Brownian motion features sub- or superexponential ensemble- but linear time-averaged mean-squared displacements *Phys. Rev. E* **103** 062127
- [168] Black F 1976 Studies of stock price volatility changes *Proc. 1976 Meetings of the Business and Economics* (American Statistical Association) pp 177–81
- [169] Schwert G W 1990 Stock volatility and the crash of '87 *Rev. Financ. Stud.* **3** 77
- [170] Bouchaud J-P 2002 An introduction to statistical finance *Physica A* **313** 238
- [171] Bouchaud J-P, Matacz A and Potters M 2001 Leverage effect in financial markets: the retarded volatility model *Phys. Rev. Lett.* **87** 228701
- [172] Gopikrishnan P, Plerou V, Nunes Amaral L A, Meyer M and Stanley H E 1999 Scaling of the distribution of fluctuations of financial market indices *Phys. Rev. E* **60** 5305
- [173] Liu Y, Gopikrishnan P, Cizeau P, Meyer M, Peng C K and Stanley H E 1999 Statistical properties of the volatility of price fluctuations *Phys. Rev. E* **60** 1390
- [174] Bassler K E, McCauley J L and Gunaratne G H 2007 Nonstationary increments, scaling distributions, and variable diffusion processes in financial markets *Proc. Natl Acad. Sci.* **104** 17287
- [175] Hua J-C, Chen L, Falcon L, McCauley J L and Gunaratne G H 2015 Variable diffusion in stock market fluctuations *Physica A* **419** 221
- [176] Chen L, Bassler K E, McCauley J L and Gunaratne G H 2017 Anomalous scaling of stochastic processes and the Moses effect *Phys. Rev. E* **95** 042141
- [177] Cont R 2001 Empirical properties of asset returns: stylized facts and statistical issues *Quant. Finance* **1** 223
- [178] Bakshi G, Cao C and Chen Z 1997 Empirical performance of alternative option pricing models *J. Finance* **52** 2003
- [179] Müller U A, Dacorogna M M, Davé R D, Olsen R B, Pictet O V and von Weizsäcker J E 1997 Volatilities of different time resolutions—analyzing the dynamics of market components *J. Empir. Finance* **4** 213
- [180] Engle R F 1982 Autoregressive conditional heteroscedasticity with estimates of the variance of United Kingdom inflation *Econometrica* **50** 987
- [181] Bollerslev T 1986 Generalized autoregressive conditional heteroskedasticity *J. Econom.* **31** 307
- [182] Andersen T G and Bollerslev T 1998 Deutsche Mark–Dollar volatility: intraday activity patterns, macroeconomic announcements, and longer run dependencies *J. Finance* **53** 219
- [183] Bollerslev T, Chou R Y and Kroner K F 1992 ARCH modeling in finance *J. Econom.* **52** 5
- [184] Francq C and Zakoian J-M 2019 *GARCH Models: Structure, Statistical Inference and Financial Applications* (New York: Wiley)
- [185] Corsi F, Mittnik S, Pigorsch C and Pigorsch U 2008 The volatility of realized volatility *Econom. Rev.* **27** 46
- [186] Andersen T G, Bollerslev T, Diebold F X and Labys P 2001 The distribution of realized exchange rate volatility *J. Am. Stat. Assoc.* **96** 42
- [187] Jiang Z-Q, Xie W-J, Zhou W-X and Sornette D 2019 Multifractal analysis of financial markets: a review *Rep. Prog. Phys.* **82** 125901
- [188] Plerou V, Gopikrishnan P, Gabaix X, Amaral L A N and Stanley H E 2001 Price fluctuations, market activity and trading volume *Quant. Finance* **1** 262
- [189] Bouchaud J-P and Potters M 2001 Welcome to a non-Black–Scholes world *Quant. Finance* **1** 482
- [190] Liu S, Oosterlee C and Bohte S 2019 Pricing options and computing implied volatilities using neural networks *Risks* **7** 16
- [191] Seemann L, McCauley J L and Gunaratne G H 2011 Intraday volatility and scaling in high frequency foreign exchange markets *Int. Rev. Financ. Anal.* **20** 121
- [192] Seemann L, Hua J-C, McCauley J L and Gunaratne G H 2012 Ensemble vs time averages in financial time series analysis *Physica A* **391** 6024
- [193] Gunaratne G H, McCauley J L, Nicol M and Török A 2005 Variable step random walks and self-similar distributions *J. Stat. Phys.* **121** 887
- [194] Mantegna R N and Stanley H E 1995 Scaling behaviour in the dynamics of an economic index *Nature* **376** 46
- [195] Mantegna R N and Stanley H E 1996 Turbulence and financial markets *Nature* **383** 587
- [196] McCauley J L 2008 Time vs ensemble averages for nonstationary time series *Physica A* **387** 5518
- [197] Redner S 1990 Random multiplicative processes: an elementary tutorial *Am. J. Phys.* **58** 267
- [198] <https://blockchain.com/charts/avg-confirmation-time>
- [199] Raberto M, Scalas E, Cuniberti G and Riani M 1999 Volatility in the Italian stock market: an empirical study *Physica A* **269** 148
- [200] Stavroyiannis S and Babalos V 2017 Herding, faith-based investments and the global financial crisis: empirical evidence from static and dynamic models *J. Behav. Finance* **18** 478